



Analysis of Scheduling Policies under Correlated Job Sizes

Varun Gupta*, Michelle Burroughs, Mor Harchol-Balter

Computer Science Department, Carnegie Mellon University, Pittsburgh, PA 15213, USA.

Abstract

Correlations in traffic patterns are an important facet of the workloads faced by real systems, and one that has far-reaching consequences on the performance and optimization of the systems involved. However, all the existing analytical work on understanding the effect of correlations between successive service requirements (job sizes) is limited to First-Come-First-Served scheduling. This leaves open fundamental questions: How do various scheduling policies interact with correlated job sizes? Can scheduling be used to mitigate the harmful effects of correlations?

In this paper we take the first step towards answering these questions. Under a simple model for job size correlations, we present the first asymptotic analysis of various common size-independent scheduling policies when the job size sequence exhibits high correlation. Our analysis reveals that the characteristics of various scheduling policies, as well as their performance relative to each other, are markedly different under the assumption of i.i.d. job sizes versus correlated job sizes. Further, among the class of size-independent scheduling policies, there is no single scheduling policy that is optimal for all degrees of correlations and thus any optimal policy must learn the correlations. We support the asymptotic analysis with numerical algorithms for exact performance analysis under an arbitrary degree of correlation, and with simulations. Finally, we verify the lessons from our correlation model on real world traces.

Keywords: Scheduling, Correlation, MMAP, $M/G/1$, Asymptotic analysis, Fluid analysis

1. Introduction

2 Motivation

3 The $M/G/1$ single-server queue has been used as a guiding model for performance analysis
4 of widely varying systems, such as buffers for network switches, web server downlinks, and the
5 CPU scheduler. There is a large body of work on the analysis of different scheduling policies and

*Corresponding author

Email addresses: varun@cs.cmu.edu (Varun Gupta), mburroug@andrew.cmu.edu (Michelle Burroughs),
harchol@cs.cmu.edu (Mor Harchol-Balter)

6 their effects on response times of jobs (defined to be the time from the arrival to the completion of
7 a job) [6]. However, almost all of the exact analysis has been performed under the assumptions
8 of (i) Poisson arrival process and (ii) independent and identically distributed (*i.i.d.*) job sizes.

9 Long ago, the need was recognized to relax these assumptions, as real systems workloads exhibit
10 significant correlation patterns, and these patterns tend to greatly affect the accuracy of the tradi-
11 tional results [9, 20]. Primarily, there are three kinds of correlations that exist in real workloads:
12 (i) correlations between consecutive interarrival times (e.g., network traffic [12], and web server
13 traffic [8, 14, 25]), (ii) correlations between interarrival times and the subsequent service require-
14 ments (e.g., [3, 5, 12, 14]), and (iii) correlations between consecutive service requirements (e.g.
15 packet sizes over network [12], supercomputing jobs [10, 16, 24], and disk request sizes [19]).
16 In this paper we focus on studying the effects of correlations of type (iii).

17 While there has been a lot of *analytical* work studying the effect of all three types of correlation
18 on mean response time in single server queues, all of this work has assumed First-Come-First-
19 Served (FCFS) queues only. Fendick et al. [12] study all three types of correlation via a Brownian
20 approximation and propose a stationary workload approximation based on heavy traffic limits.
21 Adan and Kulkarni [2] also use analysis to study autocorrelation and cross-correlation of interar-
22 rival and service times in a MAP/G/1/FCFS queue. Riska et al. [22] use matrix-analytic methods
23 to numerically calculate the mean response time in a MAP/PH/1/FCFS queue with correlated
24 arrival stream. Ghosh and Squillante [14] propose a refinement to the Fendick et al. [12] approx-
25 imation for FCFS queues, and propose approximations for a multi-class priority system with
26 FCFS scheduling within each class. Cidon et al. [5] study correlations of type (ii) by deriving
27 the Laplace transform of the workload using the theory of linear functional equations in a queue
28 with an Interrupted Poisson arrival process.

29 The effect of correlation has also been studied via *simulation*, see for example [17–19, 23, 28]. In
30 all except [18], FCFS scheduling was assumed. In [18] the authors examine an approximation of
31 Shortest-Job-First (SJF) scheduling, which the authors call SWAP, and compare it against FCFS
32 scheduling via simulation.

33 In summary, all the prior work dealing with correlations in successive job sizes has almost ex-
34 clusively dealt with FCFS scheduling. Important questions have remained unanswered: How do
35 different scheduling policies react to correlations in job sizes? Can scheduling be used to allay
36 the detrimental effect of correlated job sizes on the performance?

37 In this paper, we take an important first step by analyzing the mean response time under various
38 scheduling policies in the presence of correlated job sizes (see Table 1 for a list of policies
39 analyzed in this paper). We restrict ourselves to the class of *size-independent* policies. That is, we
40 consider policies which know the generative correlation model, but not the actual realizations of
41 the sizes (or the size-class) of jobs. In most applications, including scheduling of CPU, IP flows,
42 database queries etc., the job sizes are often not known a priori, and hence size-independent
43 policies are more realistic. We consider the question of how the optimality of size-independent
44 policies is affected by the presence or absence of correlation in the job sizes.

45 *The MMAP Correlation Model*

46 We assume the following simple *Markov Modulated Arrival Process (MMAP)* model for job-size
47 correlations: jobs belong to one of two classes called little (L) and huge (H), where jobs of class L
48 (respectively H) are Exponentially distributed with mean $\frac{1}{\mu_L}$ (respectively $\frac{1}{\mu_H} > \frac{1}{\mu_L}$)¹. Therefore,

¹Note that the mean sizes of the two classes can in fact be close. We have chosen the names of the classes to map to low (L) and high (H) load, respectively, in Section 2.

Scheduling Policy	Description
FIRST-COME-FIRST-SERVED (FCFS)	Jobs are served in the order of arrival.
LAST-COME-FIRST-SERVED (LCFS)	Whenever a job completes service, the next job to be served is the one that arrived last.
PREEMPTIVE LCFS WITH RESUME (P-LCFS)	New arrivals immediately begin service by preempting the job at the server. On a service completion, the next job to resume service is the one that arrived last.
LEAST-ATTAINED-SERVICE (LAS)	The job with the least amount of received service (age) gets to serve.
PROCESSOR SHARING (PS)	If there are n jobs in the system, each job gets $\frac{1}{n}$ th of the server's capacity.
RANDOM-ORDER-OF-SERVICE (ROS)	Whenever a job completes service, the next job to be served is picked uniformly at random from amongst the jobs currently in the queue.
OPTIMAL OMNISCIENT (OPT)	A hypothetical optimal scheduling scheme that knows the class of all jobs, and gives preemptive priority to class L jobs.

Table 1: A glossary of scheduling policies analyzed in this paper.

our jobs belong to a 2-phase hyperexponential (H_2) distribution. The system operates under a 2-state Markovian environment process with states L and H: while the environment process is in state L all arrivals are of class L, and while in state H all arrivals are of class H. The arrivals occur according to a Poisson process with rate λ independent of the environment process. The times spent in state L during each visit are *i.i.d.* Exponentially distributed with mean $\frac{1}{\alpha_L}$, and those in state H are *i.i.d.* Exponentially distributed with mean $\frac{1}{\alpha_H}$. Denote $\alpha = \alpha_L + \alpha_H$, and $p = \frac{1/\alpha_L}{1/\alpha_L + 1/\alpha_H} = \frac{\alpha_H}{\alpha}$. Thus the time-average probability of an arrival belonging to class L is p , and of belonging to class H is $1 - p$. We will use $\rho = \lambda \cdot \left(\frac{p}{\mu_L} + \frac{1-p}{\mu_H} \right)$ to denote the long run fraction of time the system is busy. If we fix the job size distribution and arrival rate (i.e. μ_L, μ_H, p, λ) and set $\alpha = \infty$, then the job sizes form an *i.i.d.* stream. As we decrease α and thereby increase the mean residence time per sojourn of L and H states, we increase the correlation among successive job sizes, since the probability that a class L job is followed by another class L job ($p_{L,L} = p + \frac{\lambda(1-p)}{\lambda+\alpha}$) increases. By expressing $p_{L,L} = \frac{\alpha}{\lambda+\alpha}p + \frac{\lambda}{\lambda+\alpha}$, we can alternately visualize the correlation model as: with probability $\frac{\lambda}{\lambda+\alpha}$ the class of a job is the same as the class of the immediately preceding job, otherwise it is an independent sample from the H_2 distribution. Let $\dots, X_{-2}, X_{-1}, X_0, X_1, X_2, \dots$ represent the sequence of job sizes. An appealing property of the above correlation model is the simple closed-form autocorrelation function (acf). In particular, the lag n correlation for $n \geq 1$ is given by:

$$\begin{aligned} \text{cor}(X_m, X_{m+n}) &= \frac{\mathbf{E}[X_m X_{m+n}] - \mathbf{E}[X_m] \mathbf{E}[X_{m+n}]}{\sqrt{\text{var}(X_m)} \sqrt{\text{var}(X_{m+n})}} = \frac{\left(\frac{\lambda}{\lambda+\alpha}\right)^n \left[\frac{p}{\mu_L^2} + \frac{1-p}{\mu_H^2} \right] + \left(1 - \left(\frac{\lambda}{\lambda+\alpha}\right)^n\right) \mathbf{E}[X_0]^2}{\text{var}(X_0)} - \frac{\mathbf{E}[X_0]^2}{\text{var}(X_0)} \\ &= \left(\frac{\lambda}{\lambda+\alpha}\right)^n \frac{\frac{\mathbf{E}[X_0^2]}{2} - \mathbf{E}[X_0]^2}{\text{var}(X_0)} = \frac{1}{2} \left(\frac{C^2 - 1}{C^2} \right) \left(\frac{\lambda}{\lambda+\alpha} \right)^n \end{aligned}$$

where $C^2 = \frac{\text{var}(X_0)}{\mathbf{E}[X_0]^2} > 1$ denotes the squared coefficient of variation (SCV) of the H_2 job size distribution.

Scope of the MMAP correlation model: The MMAP correlation model analyzed in this paper is similar to the model used in [2]. While MMAP models with more than 2 phases (e.g., [19]) or lo-

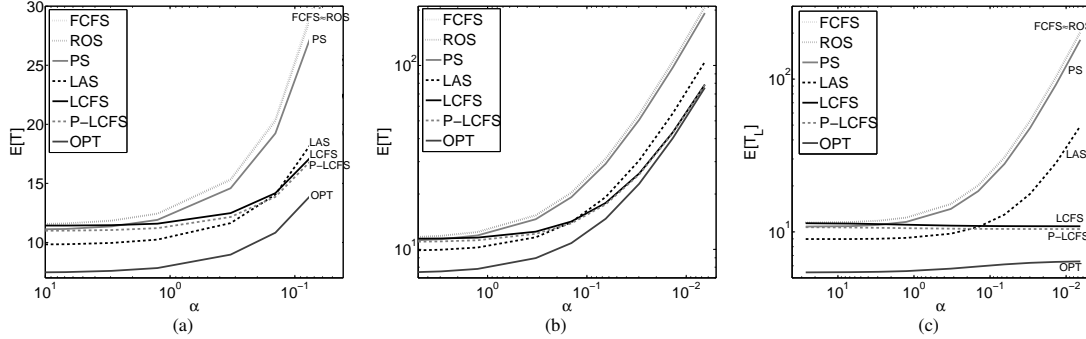


Figure 1: An example of the effect of job-size correlation on scheduling policies: (a) mean response time versus α for low to medium correlation; (b) mean response time versus α for medium to high correlation; (c) mean response time of the “little” (L) jobs versus α . Here $\rho = 0.97$ and $C^2 \approx 1.08$. Note that the $E[T]$ ordering changes from $FCFS=ROS=LCFS>PS=P-LCFS>LAS>OPT$ at $\alpha = \infty$ (*i.i.d.* job sizes) to $FCFS \approx ROS > PS > LAS > LCFS = P-LCFS = OPT$ as $\alpha \rightarrow 0$ (high correlation).

68 cal sampling based models [11] are capable of modeling more general auto-correlation functions,
 69 the goal of this paper is to use an analytically tractable correlation model to explore *qualitative*
 70 *behavior* of different scheduling policies in the presence of correlated job sizes, and to gain in-
 71 sights for these behaviors and the effect of various system parameters on the performance. We
 72 believe that the qualitative behavior of scheduling policies discovered in this paper would extend
 73 to more general correlation structures, and we partially test this via real-world traces in Section 3.

74 Summary of Contributions

75 Most of our results look at the effect of the parameter α on mean response time, $E[T]$. We
 76 prove that, although all scheduling policies we consider are hurt by increasing the correlation,
 77 the degree to which correlation affects different policies varies widely. We consider two regimes:
 78 (i) $\mu_L > \mu_H > \lambda$, where the server is never in overload, and (ii) $\mu_L > \lambda > \mu_H$, where the
 79 system is in overload during bursts of H jobs, although it is still stable on average. For the
 80 no-overload regime, we prove that, as α decreases (correlation increases), all size-independent
 81 scheduling policies become the same with respect to mean response time. For the transient-
 82 overload regime, we prove that as correlation decreases, there can be a large (up to a factor of
 83 of $\frac{\mu_L}{\mu_H}$) difference in $E[T]$ between the policies. Also, the ordering of policies from “best” to
 84 “worst” mean response time changes a lot under correlation. An example of performance of the
 85 various scheduling policies under the transient-overload regime is shown in Figure 1(a). Some
 86 particularly interesting **findings include**:

- 87 • LAS is provably sub-optimal among size-independent policies when $\alpha \rightarrow 0$, while it has
 88 provably the best mean response time when $\alpha \rightarrow \infty$ for an H_2 job size distribution (due to its
 89 decreasing failure rate [21]).
- 90 • LCFS is provably best when $\alpha \rightarrow 0$, while it is worst (along with FCFS, ROS) when $\alpha \rightarrow \infty$.
- 91 • P-LCFS is also provably best when $\alpha \rightarrow 0$, which is interesting because under $\alpha \rightarrow \infty$ (*i.i.d.*
 92 case) LCFS and P-LCFS can be far apart for high variability job size distributions.
- 93 • PS can be arbitrarily worse than P-LCFS as $\alpha \rightarrow 0$, while they are provably equal as $\alpha \rightarrow \infty$.

94 The effect of correlation on the mean response time of the L jobs, $E[T_L]$, is even more pro-
 95 nounced. In particular, we prove that:

- 96 • While $\mathbf{E}[T_L]$ increases for most policies, as α decreases (correlation increases), $\mathbf{E}[T_L]$ always
97 *decreases* for P-LCFS and for LCFS. An example is shown in Figure 1(c).
- 98 • LAS performs poorly for $\mathbf{E}[T_L]$ compared to OPT, and even worse for $\mathbf{E}[T_L^2]$. Thus, while
99 LAS is designed to help the little jobs by biasing towards jobs with least attained service, it
100 fails to do this under correlation, and policies like LCFS which are entirely oblivious to job
101 size distribution can actually help the little jobs.

102 The above results are primarily obtained by using fluid analysis and looking at asymptotic behav-
103 ior of response time as $\alpha \rightarrow 0$, see Section 2. However, the effect of correlation under moderate
104 α is also interesting. To study the moderate α regime, we derive numerical algorithms to analyze
105 LCFS, OPT, P-LCFS, and FCFS.² For the other policies, we resort to simulations, see Section 3.
106 These numerical and simulation results are useful for understanding the behavior of schedul-
107 ing policies for intermediate α values and to explore how quickly scheduling policies converge
108 to their asymptotically-limiting ($\alpha \rightarrow 0$) behavior. To see how our messages carry through to
109 real-world scenarios, we end Section 3 with trace-driven simulation studies.

110 2. Asymptotic Analysis of Scheduling Policies as $\alpha \rightarrow 0$

111 Our goal in this section is to obtain an understanding of the “first-order effect” of correlations
112 in the job sizes by considering the limiting case where the correlation approaches its maximum
113 value under our model, that is, $\alpha \rightarrow 0$.³ While this extremal case implies arbitrarily long con-
114 secutive streaks of only L and only H arrivals, an understanding of the behavior of the various
115 scheduling policies under this asymptote gives us insights into why different scheduling policies
116 react differently to correlation in job sizes, and should help guide the design of policies which
117 are robust to correlation.

118 In Section 2.1, we present the asymptotic results for the simpler case $\mu_H > \lambda$. The non-trivial
119 case of $\mu_H < \lambda$ is analyzed in Sections 2.2-2.5. A large number of scheduling policies that we
120 will analyze will involve asymptotic analysis of busy periods. We have chosen to present the
121 main results on busy period analysis in Appendix B and focus on the messages in the main body.
122 For ready reference, we have summarized the notation used in this section in Table 2.

123 *Note on scaling and asymptotic notation:*. The asymptotic analysis of the scheduling policies
124 is performed by considering a sequence of systems, indexed by the parameter α . The system
125 with index α is obtained by setting the switching rates of the environment process as $\alpha_H = p \cdot \alpha$
126 and $\alpha_L = (1 - p)\alpha$, where p, μ_L, μ_H and λ are held constant. We are interested in seeing the
127 behavior of the scheduling policies in the asymptote $\alpha \rightarrow 0$, and hence the expressions for mean
128 response times presented in this section will be written in the *asymptotic notation*: We say that
129 a function $g(\alpha)$ is of a ‘smaller order’ than $h(\alpha)$ (and make the limit $\alpha \rightarrow 0$ implicit), denoted
130 $g(\alpha) = o(h(\alpha))$, when $\frac{g(\alpha)}{h(\alpha)} \rightarrow 0$ when $\alpha \rightarrow 0$ (see Table 2). When we write the expressions
131 for the mean response time under the α th system, we only identify the dominant term in the
132 expression, expressing the remaining terms which become negligible in comparison as $\alpha \rightarrow 0$ as

²Due to lack of space, the asymptotic analysis of PS and ROS, and the results on exact numerical analysis of LCFS, OPT, P-LCFS and FCFS are presented in the extended version [15].

³The analysis of the asymptote $\alpha \rightarrow 0$ should be seen analogously to heavy traffic analysis where the traffic intensity ρ is allowed to approach 1 to observe the “first order” effect of system parameters (variance, cross-correlations) on the system performance.

Notation	Meaning	Notation	Meaning
$\mathbf{E}[T_L^\pi], \mathbf{E}[T_H^\pi], \mathbf{E}[T^\pi]$	mean response time of a class {L, H, avg} job under policy π	$\mathbf{E}[D_L^\pi], \mathbf{E}[D_H^\pi], \mathbf{E}[D^\pi]$	mean delay of a class {L, H, avg} job under scheduling policy π
$\mathbf{E}[T_L^\pi(x)], \mathbf{E}[T_H^\pi(x)]$	mean response time of a class L, H job of size x under policy π	W_L, W_H	stationary workload conditioned on being in state L, H
r_L r_H ρ	$= 1 - \frac{\lambda}{\mu_L}$ $= 1 - \frac{\lambda}{\mu_H}$ $= \lambda(p/\mu_L + (1-p)/\mu_H)$	$r_L(x)$ $r_H(x)$ $\rho(x)$	$= 1 - \lambda s_L(x)$ $= 1 - \lambda s_H(x)$ $= \lambda(p s_L(x) + (1-p) s_H(x))$
$s_L(x)$ $s_H(x)$	$= \mathbf{E}[\min\{\text{Exp}(\mu_L), x\}] = \frac{1-e^{-\mu_L x}}{\mu_L}$ $= \mathbf{E}[\min\{\text{Exp}(\mu_H), x\}] = \frac{1-e^{-\mu_H x}}{\mu_H}$	W_L^*, W_H^*	stationary fluid workload in a system with flow rates r_L and r_H , conditioned on being in state L, H
$g(x) = \Theta(h(x))$ as $x \rightarrow x_0$	$0 < \liminf_{x \rightarrow x_0} \frac{g(x)}{h(x)} \leq \limsup_{x \rightarrow x_0} \frac{g(x)}{h(x)} < \infty$	$W_L^*(x), W_H^*(x)$	stationary fluid workloads in a system with flow rates $r_L(x), r_H(x)$
$g(x) = o(h(x))$ as $x \rightarrow x_0$	$\lim_{x \rightarrow x_0} \frac{g(x)}{h(x)} = 0$	$\tilde{X}(s) = \mathbf{E}[e^{-sX}]$	Laplace transform of r.v. X

Table 2: Notation used in Section 2.

133 being of a smaller order than the dominant term. Similarly, we say $g(\alpha)$ is of ‘the same order’
134 as $h(\alpha)$ (again with the limit $\alpha \rightarrow 0$ implicit), denoted $g(\alpha) = \Theta(h(\alpha))$ when intuitively $\frac{g(\alpha)}{h(\alpha)}$
135 is eventually bounded between two strictly positive constants. Thus, for example, a $\Theta(1)$ function
136 is eventually bounded between two strictly positive constants as $\alpha \rightarrow 0$. In proving theorems
137 about response time, it will often suffice to just argue about the asymptotic order of busy period
138 durations, probabilities and related quantities.

139 2.1. Analysis for case $\mu_H > \lambda$

140 Let T_L^π and T_H^π denote the random variables for response time of class L and class H jobs, respec-
141 tively, under scheduling policy π (see Table 2). When $\mu_H > \lambda$, the system is stable during both L
142 and H states, and we have the following intuitive result which we state without proof.

143 **Theorem 1.** *Let π be any work-conserving, size-independent policy. When $\mu_H > \lambda$,*

$$\lim_{\alpha \rightarrow 0} \mathbf{E}[T_L^\pi] = \frac{1}{\mu_L - \lambda} \quad ; \quad \lim_{\alpha \rightarrow 0} \mathbf{E}[T_H^\pi] = \frac{1}{\mu_H - \lambda}.$$

144 **Remark 1:** Theorem 1 says that as job sizes become more and more correlated, the behavior of
145 all work-conserving, size-independent scheduling policies will tend to become the same, pro-
146 vided $\mu_H > \lambda$. This is because the system behaves as a mixture of two stable $M/M/1$ systems,
147 and all size-independent scheduling policies have the same mean response time for an $M/M/1$
148 system. The same argument does not apply when $\mu_H < \lambda$ because the $M/M/1$ during the H states
149 is unstable and the workload built up during the H states results in significant transient effects.

150 **Remark 2:** Since LAS is optimal (among size-independent policies) at each extreme, we intu-
151 itively expect LAS to be near-optimal through the entire range of α , and thus for all levels of
152 correlation. We verify that this is indeed true in Section 3, Figure 2.

153 2.2. Preliminaries: Workload analysis via Fluid model for the case $\mu_H < \lambda$

154 We begin our study of the case $\mu_H < \lambda$ by finding the distribution of stationary workload during
 155 the L and H states, respectively. To do this, we first introduce the *fluid model* of our MMAP
 156 correlation model.

157 **Definition 1.** Under the fluid model, we assume that the workload increases at a constant rate of
 158 $-r_H$ during the H states (see Table 2), and decreases at a constant rate of r_L during the L states
 159 as long as the workload is positive.

160 **Lemma 1.** Let W_L^* and W_H^* denote the random variables for the stationary workload during L
 161 and H states under the fluid model, respectively (we will superscript fluid model random vari-
 162 ables by *). Let $\widetilde{W}_L^*(s) = \mathbf{E}[e^{-sW_L^*}]$ and $\widetilde{W}_H^*(s) = \mathbf{E}[e^{-sW_H^*}]$ denote their Laplace transforms.
 163 Then,

$$\widetilde{W}_H^*(s) = \frac{\gamma_H - \gamma_L}{s + (\gamma_H - \gamma_L)} ; \quad \widetilde{W}_L^*(s) = \left(1 - \frac{\gamma_L}{\gamma_H}\right) + \frac{\gamma_L}{\gamma_H} \cdot \frac{\gamma_H - \gamma_L}{s + (\gamma_H - \gamma_L)}$$

164 where $\gamma_L = \frac{\alpha_L}{r_L}$ and $\gamma_H = -\frac{\alpha_H}{r_H}$.

165 Thus the workload during the H states, W_H^* , is distributed as an $\text{Exp}(\gamma_H - \gamma_L)$ random variable,
 166 and the workload during the L states, W_L^* , is a mixture of an $\text{Exp}(\gamma_H - \gamma_L)$ random variable and
 167 an atom at 0. Further, the mean of W_L^* and W_H^* are of the order $\Theta\left(\frac{1}{\alpha}\right)$. Thus, as $\alpha \rightarrow 0$, the fluid
 168 workload diverges at a rate of $\frac{1}{\alpha}$.

169 **Lemma 2.** $W_L \stackrel{d}{=} W_L^* + o(\alpha^{-1})$, $W_H \stackrel{d}{=} W_H^* + o(\alpha^{-1})$.

170 **Remark 3:** Lemma 2 says that, asymptotically as $\alpha \rightarrow 0$, the stationary workload, W_L and W_H ,
 171 of the stochastic system converge in distribution to the stationary workload, W_L^* and W_H^* , under
 172 the fluid model. While a convergence of workloads on a sample path basis was proved in [4], we
 173 are unaware of a proof of the convergence of stationary workloads.

174 **Proof of Lemma 1:** We first note that by conditional PASTA [27], W_L^* and W_H^* are equal in
 175 distribution to the stationary workload at the end of L and H states respectively. Let τ_L and τ_H
 176 be Exponentially distributed random variables with mean $\frac{1}{\alpha_L}$ and $\frac{1}{\alpha_H}$, respectively. We have the
 177 following stochastic fixed point equations:

$$W_H^* \stackrel{d}{=} W_L^* - r_H \tau_H ; \quad W_L^* \stackrel{d}{=} \max\{W_H^* - r_L \tau_L, 0\}$$

178 Taking Laplace transforms of the above equations, we get the following fixed point equations:

$$\widetilde{W}_H^*(s) = \widetilde{W}_L^*(s) \cdot \frac{\alpha_H/r_H}{\alpha_H/r_H - s}; \quad \widetilde{W}_L^*(s) = \frac{s\widetilde{W}_H^*(\alpha_L/r_L) - (\alpha_L/r_L)\widetilde{W}_H^*(s)}{s - \alpha_L/r_L},$$

which yield the expressions in Lemma 1. ■

Proof of Lemma 2: The lemma is proven by starting with Theorem 5 (Appendix A) which
 gives the exact expressions for the Laplace transforms of W_L and W_H . According to Theorem 5:

$$\widetilde{W}_L(s) = \frac{(1-\rho)\alpha m_L m_H - s m_L g_H \pi_L(0)}{\alpha_L g_H m_L + \alpha_H g_L m_H - s g_L g_H} \quad (1)$$

179 where, $m_L = \mu_L + s$, $m_H = \mu_H + s$, $g_L = \mu_L - \lambda + s$, $g_H = \mu_H - \lambda + s$, $\pi_L(0) = \frac{(1-\rho)\alpha(\mu_H + \xi)}{\xi(\mu_H - \lambda + \xi)}$, and ξ
 180 denotes the unique root of the denominator of (1) (viewed as a cubic in s) in the interval $(0, +\infty)$.

181 The quantity $\pi_L(0)$ denotes the long run fraction of time that the system is empty conditioned on
 182 being in state L. Taking the limit $\alpha \rightarrow 0$, we get

$$\xi = (\lambda - \mu_H) + \frac{p\alpha\lambda}{\lambda - \mu_H} + \Theta(\alpha^2)$$

183 and thus,

$$\pi_L(0) = \frac{(1 - \rho)\alpha(\mu_H + \xi)}{\xi(\mu_H - \lambda + \xi)} = \frac{(1 - \rho)\alpha(\lambda + \Theta(\alpha))}{(\lambda - \mu_H + \Theta(\alpha))\left(\frac{p\alpha\lambda}{\lambda - \mu_H} + \Theta(\alpha^2)\right)} = \frac{1 - \rho}{p} + \Theta(\alpha)$$

184 Note that the above is not in disagreement with the result $\Pr[W_L^* = 0] = \left(1 - \frac{\gamma_L}{\gamma_H}\right)$ as the latter is
 185 only equivalent to $\Pr[W_L = o\left(\frac{1}{\alpha}\right)]$. The other roots of the denominator of (1) in the limit $\alpha \rightarrow 0$
 186 are given by:

$$\chi = (\lambda - \mu_L) - \frac{p\alpha\lambda}{\mu_L - \lambda} + \Theta(\alpha^2) \quad \text{and} \quad \eta = -\frac{\alpha\mu_L\mu_H(1 - \rho)}{(\mu_L - \lambda)(\lambda - \mu_H)} + \Theta(\alpha^2).$$

187 Canceling the common factor $(s - \xi)$, and noting that $\frac{\alpha\mu_L\mu_H(1 - \rho)}{(\mu_L - \lambda)(\lambda - \mu_H)} = (\gamma_H - \gamma_L)$, we can rewrite:

$$\widetilde{W}_L(s) = \pi_L(0) + K_1 \frac{-\chi}{s - \chi} + K_2 \frac{-\eta}{s - \eta} = \frac{1 - \rho}{p} + K_1 \frac{\mu_L - \lambda + \Theta(\alpha)}{s + (\mu_L - \lambda + \Theta(\alpha))} + K_2 \frac{\gamma_H - \gamma_L}{s + (\gamma_H - \gamma_L)}.$$

188 Matching the coefficients of s , we get $K_1 = \frac{1 - \rho}{r_L} \left(\frac{1 - \rho}{p}\right) + \Theta(\alpha)$, and $K_2 = 1 - \frac{1 - \rho}{p r_L} + \Theta(\alpha) = \frac{\gamma_L}{\gamma_H} + \Theta(\alpha)$.
 189 Thus we have proved that, as $\alpha \rightarrow 0$, the distribution of W_L is a mixture of an Exponential distri-
 190 bution with mean $\frac{1}{\gamma_H - \gamma_L}$ with probability $\sim \frac{\gamma_L}{\gamma_H}$, and with the remaining probability the stationary
 191 distribution of an $M/M/1$ with arrival rate λ and service rate μ_L . ■

192 *Goals of asymptotic analysis.* Since we are interested in analyzing work-conserving policies,
 193 the stationary workload, W , is the same across policies. What differs from one policy to another
 194 is what types of jobs make up that work. Since we restrict ourselves to size-independent policies,
 195 we can bound the mean remaining size of any job under our H_2 job size distribution between
 196 $\frac{1}{\mu_L}$ and $\frac{1}{\mu_H}$. This gives bounds on $\mathbf{E}[N^\pi]$ – the mean number of jobs in the system for any work-
 197 conserving policy π – as $\mu_H \mathbf{E}[W] \leq \mathbf{E}[N^\pi] \leq \mu_L \mathbf{E}[W]$. Finally, by applying Little’s law, we get
 198 $\frac{\mu_H}{\lambda} \mathbf{E}[W] \leq \mathbf{E}[T^\pi] \leq \frac{\mu_L}{\lambda} \mathbf{E}[W]$. Since $\mathbf{E}[W]$ diverges as $\frac{1}{\alpha}$ as $\alpha \rightarrow 0$, we have the following.

199 **Lemma 3.** *When $\mu_H < \lambda$ in the MMAP model, the mean response time of any work-conserving*
 200 *size-independent scheduling policy π grows as $\mathbf{E}[T^\pi] = \frac{K^\pi}{\alpha} + o\left(\frac{1}{\alpha}\right)$, for some constant K^π which*
 201 *depends only on the scheduling policy and the parameters μ_H, μ_L, p and λ .*

202 Our goal is to identify the K^π for different policies. This is analogous to heavy traffic analysis,
 203 where space (response time, number of jobs in system, etc.) is scaled by $(1 - \rho)$ and analyzed in
 204 the limit $\rho \rightarrow 1$.

205 2.3. FCFS

Theorem 2. *In the regime $\mu_H < \lambda$,*

$$\mathbf{E}[D_L^{FCFS}] = \frac{(1 - \rho)}{p(1 - \rho)} \left(\frac{\lambda}{\mu_H} - 1\right)^2 \frac{1}{\alpha} + o\left(\frac{1}{\alpha}\right)$$

$$\mathbf{E}[D_H^{FCFS}] = \frac{1}{(1 - \rho)} \left(1 - \frac{\lambda}{\mu_L}\right) \left(\frac{\lambda}{\mu_H} - 1\right) \frac{1}{\alpha} + o\left(\frac{1}{\alpha}\right)$$

206 **Proof:** By conditional PASTA, the delay of class L jobs is distributed as W_L , and that of class H
207 as W_H . Applying Lemmas 2 and 1, the result is immediate. ■

208 **Remark 4:** We already see a divergence in the behavior of scheduling policies when job sizes
209 become correlated. When $\alpha \rightarrow \infty$ (*i.i.d.* case), and under a Poisson arrival process, the mean
210 delay under FCFS depends only on the first two moments of the job size distribution. However,
211 as $\alpha \rightarrow 0$, it depends on all the parameters of the H_2 job size distribution.

212 2.4. OPT, P-LCFS and LCFS

213 While it is hard to characterize the optimal size-independent policy when job sizes are correlated
214 since the optimal policy might (and will) exploit the correlation structure to predict classes of
215 future jobs based on observed history of job sizes, a trivial lower bound is obtained by considering
216 an omniscient scheduler – that is, a scheduler that knows the *class* (L,H) of each job in the system,
217 but not the exact size, and gives preemptive priority to class L jobs. We call this policy OPT.

Theorem 3. When $\mu_H < \lambda$, we have for each policy $\pi \in \{OPT, P-LCFS, LCFS\}$:

$$\begin{aligned} \mathbf{E}[D_L^\pi] &= \Theta(1) \\ \mathbf{E}[D_H^\pi] &= \left[\frac{\mu_H}{\lambda(1-p)} \right] \frac{(1-p)\lambda}{(1-\rho)} \left(\frac{1}{\mu_H} - \frac{1}{\mu_L} \right) \left(\frac{\lambda}{\mu_H} - 1 \right) \frac{1}{\alpha} + o\left(\frac{1}{\alpha}\right) \end{aligned}$$

218 **Corollary 1.** For $\pi \in \{LCFS, P-LCFS, OPT\}$, when $\mu_H < \lambda$: $\lim_{\alpha \rightarrow 0} \frac{\mathbf{E}[T^{FCFS}]}{\mathbf{E}[T^\pi]} = \frac{\lambda}{\mu_H}$.

219 **Proof of Theorem 3:** We first consider class L jobs. Under OPT, class L jobs get priority, and
220 hence their response time is stochastically upper bounded by that of an $M/M/1$ with arrival rate
221 λ and service rate μ_L , and is $\Theta(1)$. Under P-LCFS, the response time of class L jobs is the busy
222 period started by $\text{Exp}(\mu_L)$ work in state L. By Theorem 6, Case 2 (see Appendix B), this is $\Theta(1)$.
223 Under LCFS, the delay of class L jobs is a busy period started either by $\text{Exp}(\mu_L)$, $\text{Exp}(\mu_H)$ or 0
224 work. Again, by Theorem 6, Case 2, this is $\Theta(1)$.

225 To understand the delay of class H jobs, note that the above implies that the mean number of
226 class L jobs in the system, and hence their contribution to the total workload is $\Theta(1)$. However,
227 the stationary average workload is $\Theta(\alpha^{-1})$, and hence this must be composed (aside from a $\Theta(1)$
228 term) of class H jobs alone. Since, all scheduling policies are size-independent, the mean resid-
229 ual size of these class H jobs is $\frac{1}{\mu_H}$, yielding the mean number of class H jobs of $\frac{p\mathbf{E}[W_L] + (1-p)\mathbf{E}[W_H]}{1/\mu_H}$.

230 By Little's law, we obtain the mean delay of class H jobs as $\frac{p\mathbf{E}[W_L] + (1-p)\mathbf{E}[W_H]}{\lambda(1-p)/\mu_H}$. ■

231 **Remark 5:** The proof does not extend to other policies in Table 1 as their $\mathbf{E}[T_L]$ is not $\Theta(1)$.

232 **Remark 6:** For the metric of $\mathbf{E}[T]$, all three policies – OPT, P-LCFS and LCFS – are asymptot-
233 ically optimal. However, $\mathbf{E}[T_L]$ under the three policies is different, although always $\Theta(1)$, and
234 given by the following lemma, whose proof we omit.

Lemma 4. When $\mu_H < \lambda$, $\mathbf{E}[T_L]$ under OPT, LCFS and P-LCFS are given by:

$$\begin{aligned} \mathbf{E}[T_L^{OPT}] &= \frac{1}{\mu_L - \lambda} + o(1) \\ \mathbf{E}[T_L^{P-LCFS}] &= \mathbf{E}[B_L^L] + o(1) = \frac{1 - \rho_H}{\mu_L(1 - \rho)} + o(1) \\ \mathbf{E}[T_L^{LCFS}] &= \theta_H \left(1 - \frac{\lambda}{\mu_L}\right) \mathbf{E}[B_L^H] + \frac{\lambda}{\mu_L} \mathbf{E}[B_L^L] + \frac{1}{\mu_L} + o(1) \end{aligned}$$

235 where $\theta_H = \frac{(1-p)(\lambda - \mu_H)}{(1-p)\lambda + (p-\rho)\mu_H}$, and $\mathbf{E}[B_L^L]$ and $\mathbf{E}[B_L^H]$ are given in Corollary 2 (see Appendix B).

236 **Remark 7:** Comparing with $\mathbf{E}[T_L^{P-LCFS}]_{\alpha \rightarrow \infty} = \frac{1}{\mu_L} \cdot \frac{1}{1-\rho}$, we see that the extreme correlated $\mathbf{E}[T_L]$
 237 for P-LCFS is always lower than the uncorrelated $\mathbf{E}[T_L]$. We can prove a similar result for LCFS.

238 **Remark 8:** A further difference between the three policies emerges if one looks at higher order
 239 metrics, such as $\mathbf{E}[(T_L^x)^2]$. As a byproduct of the proof of Theorem 6 (Case 2), we can see
 240 that $\mathbf{E}[(T_L^{P-LCFS})^2] = \Omega(\frac{1}{\alpha})$, while it is $\Theta(1)$ for OPT. Thus, while simple policies such as P-
 241 LCFS and LCFS are asymptotically optimal for $\mathbf{E}[T]$, learning-based scheduling policies might
 242 be preferred when one cares about more fine-grained metrics.

243 2.5. LAS

244 The asymptotic analysis of LAS presented below builds on the analysis under *i.i.d.* arrivals given
 245 in [7]. In short, to analyze the response time of a tagged arrival of size x , we consider a modified
 246 system where jobs of original size s are truncated to size $\min\{s, x\}$ when they enter the system.
 247 Under LAS, the response time of the tagged arrival is given by the busy period generated by the
 248 work it sees on arrival in this modified system.

249 **Theorem 4.** *When $\mu_H < \lambda$, the mean response time of a job of size x under the LAS scheduling*
 250 *policy is given by:*

251 **Case $\lambda s_H(x) > 1$:**

$$\mathbf{E}[T_L^{LAS}(x)] = \frac{\mathbf{E}[W_L^*(x)]}{1 - \rho(x)} + o\left(\frac{1}{\alpha}\right); \quad \mathbf{E}[T_H^{LAS}(x)] = \frac{1}{\alpha_H} + \frac{\mathbf{E}[W_H^*(x)] + \frac{\lambda s_H(x) - 1}{\alpha_H}}{1 - \rho(x)} + o\left(\frac{1}{\alpha}\right)$$

252 **Case $\lambda s_H(x) < 1$:**

$$\mathbf{E}[T_L^{LAS}(x)] = \mathbf{E}[T_L^{M/M/1/LAS}(x)] + o(1); \quad \mathbf{E}[T_H^{LAS}(x)] = \mathbf{E}[T_H^{M/M/1/LAS}(x)] + o(1)$$

253 where $\mathbf{E}[T_L^{M/M/1/LAS}(x)]$ and $\mathbf{E}[T_H^{M/M/1/LAS}(x)]$ denote the mean response time of a job of size x
 254 under LAS scheduling in $M/M/1$ queues with arrival rate λ , and job size distribution $\text{Exp}(\mu_L)$
 255 and $\text{Exp}(\mu_H)$, respectively.

256 **Proof: Case $\lambda s_H(x) > 1$:** In this case, the modified system with truncated job sizes is in transient
 257 overload during the H states. Theorem 6, Case 1 (see Appendix B), gives us the expression for
 258 the required mean busy period.

259 **Case $\lambda s_H(x) < 1$:** In this case, the modified system with truncated job sizes is stable during the
 260 H states. As $\alpha \rightarrow 0$, the system looks like a mixture of two independent stable $M/G/1$ queues
 261 with the modified job size distributions (similar to Theorem 1). The mean response time of a
 262 type L job of size x in this modified system thus converges to the mean response time of a job of
 263 size x under an $M/M/1/LAS$ system with arrival rate λ and job sizes *i.i.d.* $\text{Exp}(\mu_L)$. A similar
 264 argument applies to type H jobs of size x . ■

265 **Remark 9:** Under *i.i.d.* H_2 job sizes, LAS is the optimal size-independent policy for minimizing
 266 $\mathbf{E}[T]$ because it isolates the class L jobs from class H jobs. Intuitively we expect this behavior to
 267 carry over when correlations are introduced, *but this is not the case*. Not only does LAS perform
 268 suboptimally, but $\mathbf{E}[T_L]$ under LAS grows as $\Theta(\frac{1}{\alpha})$, while it is $\Theta(1)$ under LCFS and P-LCFS.
 269 The reason for this counter-intuitive behavior lies in the fraction of L jobs that do not get isolation
 270 and hence experience $\Theta(\frac{1}{\alpha})$ mean response time. Under LCFS and P-LCFS, this fraction is $\Theta(\alpha)$
 271 with a net effect of $\Theta(1)$. Under LAS, however, all L jobs with a size bigger than $\frac{1}{\mu_H} \log\left(\frac{\mu_H}{\lambda - \mu_H}\right)$,
 272 which is a $\Theta(1)$ fraction, experience $\Theta(\frac{1}{\alpha})$ mean response time.

273 3. Evaluation via Simulations

274 While Section 2 provided fluid asymptotics as $\alpha \rightarrow 0$ for a wide range of size-independent
 275 scheduling policies, we are only able to perform exact numerical analysis of the case $0 < \alpha < \infty$
 276 for a smaller subset (FCFS, LCFS, P-LCFS, OPT) via algorithms proposed in the supplement
 277 [15]. This section studies the full range of policies for all α via numerical techniques for the
 278 policies mentioned above, and via simulation for the remaining policies in Table 1. We start with
 279 results for our MMAP model and then present results for trace-based experiments.

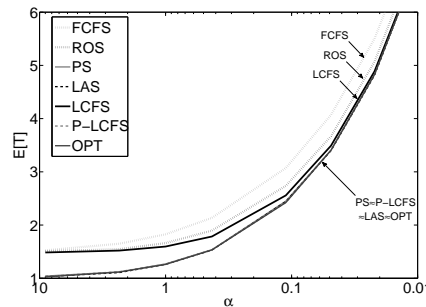


Figure 2: Effect of job size correlation when $\mu_H > \lambda$. The parameters chosen were $\mu_L = 50.73, \mu_H = 1.0055, p = 0.5073, \lambda = 1$ ($\rho = 0.5, C^2 \approx 2.9$).

280 **MMAP under No transient overload:** In Figure 2, we see the effect of correlation on scheduling
 281 policies when $\mu_H > \lambda$, so that there is no transient overload in H states. We see that for moderate
 282 α , $\mathbf{E}[T]$ of the different scheduling policies range from $\mathbf{E}[T] = 1$ to about $\mathbf{E}[T] = 1.5$, with FCFS
 283 being the worst and LAS being the best. As α decreases, we see that the relative performance
 284 difference between scheduling policies begin to vanish ($\mathbf{E}[T]$ ranges from 6.9 to 7.5 for $\alpha \approx$
 285 0.01). This behavior as $\alpha \rightarrow 0$ is consistent with Theorem 1. Observe also that while FCFS,
 286 ROS and LCFS are equal at the two extremes ($\alpha \rightarrow \infty$ and $\alpha \rightarrow 0$), for $0 < \alpha < \infty$ they are
 287 ordered as $\text{FCFS} > \text{ROS} > \text{LCFS}$ with respect to $\mathbf{E}[T]$.

288 **MMAP under Transient overload:** Figure 3 shows the effect of correlation in the more inter-
 289 esting case of $\mu_H < \lambda$, implying that there is transient overload during the H states. Figure 3(a)
 290 shows the $\mathbf{E}[T]$ vs. α curves for the different scheduling policies. We see that FCFS is the worst
 291 policy and LAS is optimal or close to optimal throughout the range of α shown. On the other
 292 hand, P-LCFS starts out equal to PS when $\alpha \rightarrow \infty$ and is clearly suboptimal; yet for low α (high
 293 correlation), P-LCFS approaches and even overtakes LAS, and becomes optimal. This is consis-
 294 tent with Theorem 3. Similarly, LCFS starts out equal to FCFS when $\alpha \rightarrow \infty$ and is worst in
 295 performance, but becomes optimal as $\alpha \rightarrow 0$, again confirming Theorem 3.

296 A major difference between Figure 3(a) (transient overload) and Figure 2 (no overload) is that the
 297 policies clearly do not converge to each other in Figure 3 as $\alpha \rightarrow 0$, whereas they do in Figure 2.
 298 Furthermore, for each policy π in Figure 3(a), the $\mathbf{E}[T]$ curve asymptotes to a line on the plotted
 299 scale, which corresponds to $\mathbf{E}[T^\pi] \sim \frac{K^\pi}{\alpha}$ as in Lemma 3. Thus the mean response times grow
 300 unboundedly as $\alpha \rightarrow 0$, unlike in Figure 2.

301 Figure 3(b) verifies the expressions for K^π obtained from our asymptotic analysis by showing
 302 $\left(\frac{\alpha}{1+\alpha}\right)\mathbf{E}[T]$ as a function of $\frac{1}{1+\alpha}$. We choose to scale $\mathbf{E}[T]$ by $\frac{\alpha}{1+\alpha}$ (instead of α) to show the
 303 results for $\alpha \rightarrow \infty$ asymptote and the $\alpha \rightarrow 0$ asymptote in the same plot. In the former case,
 304 $\lim_{\alpha \rightarrow \infty} \frac{\alpha}{1+\alpha}\mathbf{E}[T^\pi] = \lim_{\alpha \rightarrow \infty} \mathbf{E}[T^\pi]$ and in the latter case $\lim_{\alpha \rightarrow 0} \frac{\alpha}{1+\alpha}\mathbf{E}[T^\pi] = \lim_{\alpha \rightarrow 0} \alpha\mathbf{E}[T^\pi] =$

305 K^π . The x -axis shows $\frac{1}{1+\alpha}$ which is bounded between 0 and 1 (unlike α). The $\alpha E[T^\pi]$ curves
 306 clearly converge to the analytically obtained values of K^π marked with a small x . In the limit
 307 $\alpha \rightarrow 0$, $E[T]$ for the different policies follows the order LCFS = P-LCFS < LAS < PS < ROS <
 308 FCFS. Due to the parameter settings, the difference between LAS and LCFS = P-LCFS as $\alpha \rightarrow 0$
 is very slight; this contrasts with Figure 1 where the difference was significant.

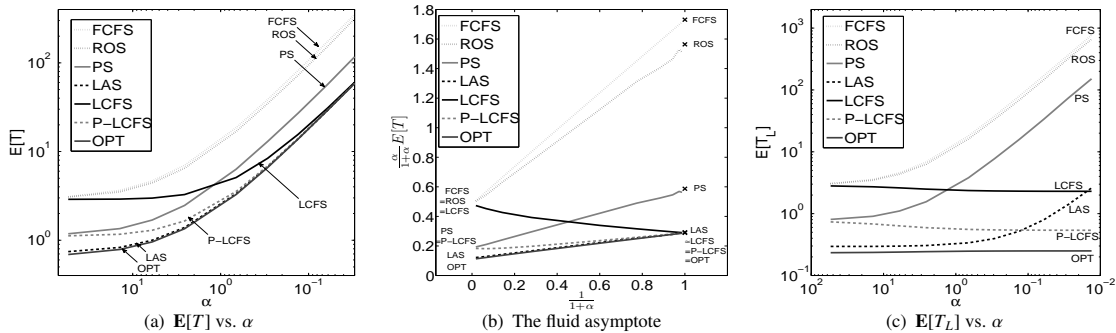


Figure 3: Effect of job size correlation when $\mu_H < \lambda$. The parameters chosen were $\mu_L = 10, \mu_H = 1, p = 0.95, \lambda = 6$ ($\rho = 0.87, C^2 \approx 4.66$).

309 Figure 3(c) shows mean response time for “little” (class L) jobs, denoted $E[T_L]$, versus α . For the
 310 L jobs, there is a wide difference (several orders of magnitude) in performance across policies.
 311 Several policies (FCFS, ROS, PS, LAS) show $E[T_L]$ increasing in proportion to $\frac{1}{\alpha}$ (though this
 312 is less obvious in the case of LAS); however, other policies (LCFS, P-LCFS) show a decrease in
 313 $E[T_L]$ as α decreases, as pointed out in Remark 7. Under the first group of policies, $E[T_L]$ suffers
 314 from increased correlation, because L jobs are affected by H jobs. For LCFS and P-LCFS, this
 315 is not the case, since an L job is only affected by H jobs if they arrive during the L job’s busy
 316 period. This happens with probability proportional to α , which becomes zero as $\alpha \rightarrow 0$.

317 **Trace-based experiments:** While we garnered useful intuition by analyzing the MMAP correlation
 318 model, it is not obvious to what extent our results would extend to real-world applications.
 319 To investigate this, we consider two very different traces, one involving packets sizes (Bellcore)
 320 and a second involving supercomputing job sizes (SHARCNET). We have simulated FCFS, ROS,
 321 PS, LCFS and P-LCFS policies. In addition, we simulate PRIO-P, which gives preemptive priority
 322 to class L jobs, where class L jobs are defined as jobs with size below some threshold.
 323 Hence the PRIO-P policy is similar to the OPT policy, but is not necessarily the optimal size-
 324 independent policy because class L and H jobs are no longer Exponentially distributed. We also
 325 simulate SRPT (Shortest Remaining Processing Time) policy, and our plots show $E[T]$ under the
 326 simulated policies normalized by the mean response time under SRPT scheduling.
 327

328 Figures 4(a)-4(d) show the results of our experiments with a trace of packet sizes seen on the
 329 Bellcore Ethernet [13]. The autocorrelation function of packet sizes (Figure 4(a)) shows signif-
 330 icant sequential job size correlation – the lag-1 correlation is approximately 0.45 with correla-
 331 tion persisting even at lags of up to 100 (unlike MMAP model where the correlation decreases
 332 exponentially in lag). Figure 4(b) shows the job size distribution which is almost a trimodal
 333 distribution. To perform the simulations, we modify the base trace as follows: In the first set of
 334 experiments (Figure 4(c)), we scale the interarrival times from the trace to vary the ‘load’. In the
 335 second set of experiments (Figure 4(d)), we keep the same sequence of job sizes as the original
 336 trace, but create a new Poisson arrival process to eliminate correlations in the arrival process

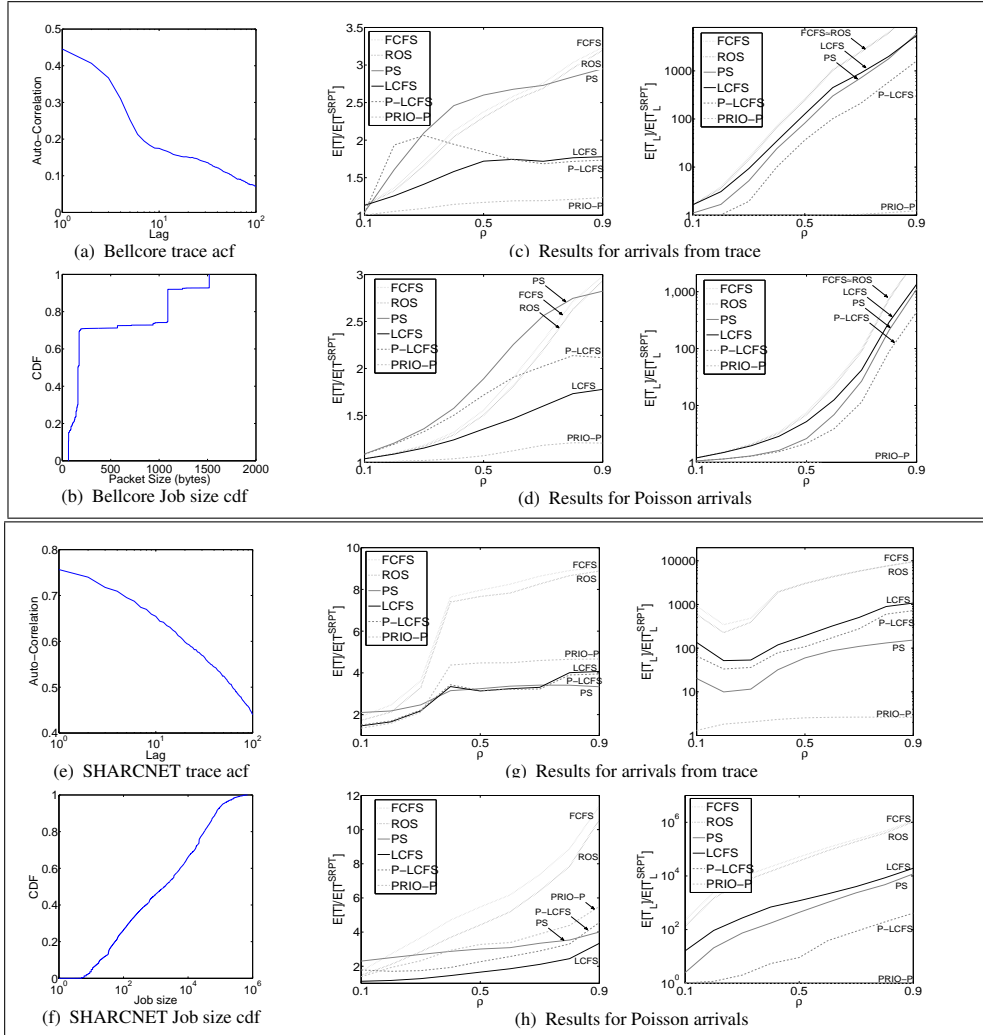


Figure 4: Trace-based experiments. Simulation results for the Bellcore trace are shown in the top box, and for the SHARCNET trace in the bottom box. For each set of traces, the top-left plot shows the autocorrelation function for job size sequence; the bottom-left plot shows the cdf of the job size distribution; the two top-right plots show the performance (as the ratio of $E[T]$ to $E[T^{SRPT}]$, and of $E[T_L]$ to $E[T_L^{SRPT}]$, respectively) when the interarrival times are taken from the trace; the two bottom right plots show the performance obtained by creating a synthetic Poisson arrival process.

337 (the trace arrival process is bursty) and correlations between interarrival times and job sizes (the
 338 correlations between a job size and immediately following interarrival time is -0.15). We see
 339 that with respect to $E[T]$, the ordering of the policies largely obeys $FCFS \approx ROS \approx PS > LCFS \approx P-$
 340 $LCFS > PRIO-P > SRPT$. This is consistent with the ordering we obtained via analysis using the
 341 MMAP correlation model. We also see that $E[T^{FCFS}]$ is up to 1.8 times worse than $E[T^{LCFS}]$
 342 which contrasts with the uncorrelated case where they are equal. We also investigate the effect
 343 of scheduling on the little jobs by classifying packets of size less than 400 bytes as L. Under
 344 our criterion, the L jobs make up 70% of the packets, and 25% of the total bytes. We find that

$\mathbf{E}[T_L^{FCFS}]$ is up to 3 to 4 times worse than $\mathbf{E}[T_L^{LCFS}]$ and almost 10 times worse than $\mathbf{E}[T_L^{P-LCFS}]$. We also see that PS outperforms LCFS but not P-LCFS in terms of $\mathbf{E}[T_L]$. This can be explained by the fact that under the uncorrelated case PS and P-LCFS have identical performance and outperform LCFS which suffers due to job size variability. Under moderate correlation, we see a behavior that is the mixture of uncorrelated and high-correlation cases: job size variability is still hurting class L jobs under LCFS and thus gives them worse performance than PS, however due to correlation P-LCFS is able to perform better than PS (our MMAP simulation results also suggest that for moderate correlations, PS still outperforms LCFS). The same observations hold under a Poisson arrival process, but the gains are more moderate. This suggests that in the presence of cross-correlations and bursty arrivals, the effect of scheduling will be more pronounced. Figures 4(e)-4(h) show the results for the SHARCNET trace [1], which is a supercomputing workload. Here job size is defined as the run time of jobs submitted to the server, and the correlation in the sequence of job sizes is very high (lag-1 autocorrelation is over .7, and even lag-100 correlation is over .4). The ordering of policies with respect to $\mathbf{E}[T]$ largely obeys $FCFS > ROS > PRIO-P > PS \approx P-LCFS \approx LCFS > SRPT$. The gains of utilizing LCFS instead of FCFS for the SHARCNET trace are even more significant, as the ratio of $\mathbf{E}[T^{FCFS}]$ to $\mathbf{E}[T^{LCFS}]$ can be over 2. For the SHARCNET trace, we defined L jobs as those smaller than 54000 seconds (86% jobs, 25% of total load). There is again a significant difference between $\mathbf{E}[T_L^{FCFS}]$ and $\mathbf{E}[T_L^{LCFS}]$, up to 4X when scaling the original interarrival times, and 15X to 20X when the arrival process has been converted to a Poisson process. Comparing $\mathbf{E}[T_L]$ for LCFS, PS and P-LCFS, we see that PS does better than LCFS which can be explained by the presence of job size variability. However the ordering of PS and P-LCFS under arrival times from the SHARCNET trace switches when a Poisson arrival process is considered. While under a Poisson arrival process, PS performs worse than P-LCFS as predicted by our analysis of the MMAP correlation model, under the arrival sequence from the SHARCNET trace, PS outperforms P-LCFS. This suggests that the correlation between the arrival times (the SHARCNET arrival sequence has extremely bursty and variable interarrival times compared to the Bellcore trace) is also an important aspect to consider to fully understand the effect of scheduling under correlated traffic pattern.

373 4. Conclusions

374 To the best of our knowledge, this is the first paper to study analytically how common scheduling
 375 policies, like PS, LAS, ROS, P-LCFS, LCFS, etc. are affected by correlation among consecutive
 376 job sizes. We find the ranking of scheduling policies, from highest to lowest mean response
 377 time ($\mathbf{E}[T]$), changes dramatically under correlation: LCFS which performs poorly under no
 378 correlation becomes optimal among size-independent policies under high correlation; the optimal
 379 size-independent policy for i.i.d. job sizes, LAS, becomes sub-optimal under high correlation;
 380 the mean response times of policies which are insensitive to job-size variability when job sizes
 381 are i.i.d., like PS and P-LCFS, now depend on the entire job-size distribution, to cite a few
 382 examples. When examining the mean response time of “little” jobs only ($\mathbf{E}[T_L]$), the change in
 383 ranking is even more dramatic, with correlation actually making some policies like LCFS and
 384 P-LCFS perform better, and making other policies like LAS perform far worse.
 385 We have only scratched the surface of how correlation in job sizes affects performance. First, our
 386 correlation model is very simple, chosen for analytical tractability and to gain insights; extending
 387 the results presented here to richer models is left for future work. Second, while this paper
 388 shows that P-LCFS and LCFS perform optimally among size-independent policies under very

389 high correlation, the paper does not answer the question of which policy is best under moderate
 390 correlation. Furthermore, we have not even explored policies which might exploit the correlation
 391 structure to improve performance. Third, our model only captures correlations in consecutive
 392 job sizes, but we believe that the techniques introduced herein can be applied to understanding
 393 the effect of all three types of correlation on the performance of scheduling policies.

394 Appendix A. Transforms for stationary workload

Theorem 5. Let $\widetilde{W}_L(s)$ and $\widetilde{W}_H(s)$ denote the transform for the stationary workloads during the L and H states, respectively, under the MMAP model. Then:

$$\widetilde{W}_L(s) = \frac{(1 - \rho)\alpha m_L m_H - s m_L g_H \pi_L(0)}{\alpha_L g_H m_L + \alpha_H g_L m_H - s g_L g_H} \quad (\text{A.1})$$

where,

$$\begin{aligned} m_L = \mu_L + s & \quad ; \quad m_H = \mu_H + s \\ g_L = \mu_L - \lambda + s & \quad ; \quad g_H = \mu_H - \lambda + s \end{aligned} \quad ; \quad \pi_L(0) = \frac{(1 - \rho)\alpha(\mu_H + \xi)}{\xi(\mu_H - \lambda + \xi)}$$

395 and ξ denotes the unique root of the denominator of (A.1) in the interval $(0, +\infty)$. The quantity
 396 $\pi_L(0)$ denotes the long run fraction of time that the system is empty conditioned on being in state
 397 L. The expression for $\widetilde{W}_H(s)$ is obtained by flipping μ_H and μ_L , and flipping α_L and α_H .

398 **Proof:** The first step is analysis of the transient workload in an $M/G/1$. Consider an $M/G/1$
 399 with arrival rate λ , *i.i.d.* job sizes X_1, X_2, \dots with Laplace transform of the job size distribution
 400 given by $\mathbf{E}[e^{-sX_1}] = \widetilde{X}(s)$. We can write the following equation for the evolution of the workload
 401 $W(t)$ in this $M/G/1$:

$$W(t + \delta t) = W(t) - \delta t \mathbf{1}_{W(t) > 0} + \sum_n X_n \mathbf{1}_{n\text{th arrival in } (t, t + \delta t)}$$

402 Let $\widetilde{W}_t(s) = \mathbf{E}[e^{-sW(t)}]$. Taking Laplace transforms in the above equation, and then letting $\delta t \rightarrow 0$,

$$\frac{d}{dt} \widetilde{W}_t(s) = \widetilde{W}_t(s) (s - \lambda(1 - \widetilde{X}(s))) - s \Pr[W_t = 0]$$

Let T be an $\text{Exp}(\nu)$ random variable and $\widetilde{W}_T(s) = \mathbf{E}[e^{-sW(T)}]$. Using integration by parts, we get:

$$\begin{aligned} \widetilde{W}_T(s) &\equiv \int_{u=0}^{\infty} \widetilde{W}_u(s) \nu e^{-\nu u} du = \left[\frac{\widetilde{W}_u(s) \nu e^{-\nu u}}{-\nu} \right]_{u=0}^{\infty} + \int_{u=0}^{\infty} \frac{d\widetilde{W}_u(s)}{du} e^{-\nu u} du \\ &= \widetilde{W}_0(s) + \frac{1}{\nu} \int_{u=0}^{\infty} (\widetilde{W}_u(s) [s - \lambda(1 - \widetilde{X}(s))] - s \Pr[W_u = 0]) \nu e^{-\nu u} du \\ &= \widetilde{W}_0(s) + \frac{1}{\nu} (\widetilde{W}_T(s) [s - \lambda(1 - \widetilde{X}(s))] - s \Pr[W(T) = 0]) \end{aligned}$$

Specializing to our problem, we obtain the following two relations by applying the above equation during L and H states, and noting that by PASTA $\widetilde{W}_L(s)$ and $\widetilde{W}_H(s)$ also denote the stationary workloads at the *ends* of L and H states, respectively:

$$\widetilde{W}_L(s) = \widetilde{W}_H(s) + \frac{s}{\alpha_L} \left[\widetilde{W}_L(s) \left(1 - \frac{\lambda}{\mu_L + s} \right) - \pi_L(0) \right]$$

$$\widetilde{W}_H(s) = \widetilde{W}_L(s) + \frac{s}{\alpha_H} \left[\widetilde{W}_H(s) \left(1 - \frac{\lambda}{\mu_H + s} \right) - \pi_H(0) \right]$$

403 Eliminating $\widetilde{W}_H(s)$, and $\pi_H(0)$ by using the fact $\frac{\pi_L(0)}{\alpha_L} + \frac{\pi_H(0)}{\alpha_H} = (1 - \rho) \left(\frac{1}{\alpha_L} + \frac{1}{\alpha_H} \right)$, we obtain
 404 the expression for $\widetilde{W}_L(s)$ shown in the Theorem. It now remains to determine the unknown
 405 $\pi_L(0)$. To obtain this, we note that the polynomial in the denominator of $\widetilde{W}_L(s)$ is a cubic in s
 406 which approaches $-\infty$ as $s \rightarrow \infty$. Further, the denominator is positive at $s = 0$ but negative at
 407 $s = \lambda - \mu_L < 0$. Therefore there is exactly one root of the denominator in the interval $(0, +\infty)$,
 408 which we denote by ξ , at which there is a degeneracy in the denominator. Since the transform
 409 must converge in $Re(s) > 0$, the numerator must share this root, yielding the unknown $\pi_L(0)$. ■

410 Appendix B. Asymptotic Expressions for Mean Busy Periods

411 Busy periods form the core of the analysis for scheduling policies, and therefore we deal with
 412 the problem of analyzing busy periods in as much generality as possible.

413 We consider a system with an environment controlled by a 2-state Markov chain with states L and
 414 H. The time spent in state L during each visit is $\text{Exp}(\alpha_L)$ and time spent in state H is $\text{Exp}(\alpha_H)$.
 415 Let $\alpha = \alpha_L + \alpha_H$, $p = \frac{\alpha_H}{\alpha}$. The arrivals occur at a rate λ in each state. The arrivals during an L
 416 state have *i.i.d.* general job sizes and are denoted by random variable S_L . Similarly, the arrivals
 417 during an H state have *i.i.d.* general job sizes denoted by random variable S_H . We will assume
 418 $\mathbf{E}[S_L] < \mathbf{E}[S_H]$. We index this system by α .

419 **The scaling:** We consider a sequence of systems, indexed by α , obtained by setting the switching
 420 rates as $\alpha_L + \alpha_H = \alpha$, while fixing $p = \frac{\alpha_H}{\alpha}$. We start the α th system in a prescribed state with
 421 initial workload (a random variable) denoted by W_α . We will say that the workload sequence
 422 W_α is $\Theta(g(\alpha))$ if the sequence $\left\{ \frac{W_\alpha}{g(\alpha)} \right\}$ is uniformly integrable and $\lim_{\alpha \rightarrow 0} \frac{W_\alpha}{g(\alpha)} \xrightarrow{d} \overline{W}$, where \overline{W} is
 423 some non-degenerate random variable. Similarly, we say $W_\alpha = o(h(\alpha))$ if $W_\alpha = \Theta(g(\alpha))$ and
 424 $\lim_{\alpha \rightarrow 0} \frac{g(\alpha)}{h(\alpha)} = 0$, or $W_\alpha = \omega(h(\alpha))$ if $W_\alpha = \Theta(g(\alpha))$ and $\lim_{\alpha \rightarrow 0} \frac{h(\alpha)}{g(\alpha)} = 0$.

425 **Goal:** Let $B_L(W_\alpha)$ and $B_H(W_\alpha)$ denote the random variables for the busy periods started by work
 426 W_α in states L and H, respectively, in the α th system. We will be interested in obtaining the mean
 427 busy period in the asymptotic regime $\alpha \rightarrow 0$. That is, we are interested in obtaining the dominant
 428 term in $\mathbf{E}[B_L(W_\alpha)]$ or $\mathbf{E}[B_H(W_\alpha)]$, as the switching rate $\alpha \rightarrow 0$.

Notation: $\widetilde{S}_L(s) = \mathbf{E}[e^{-sS_L}]$; $\widetilde{S}_H(s) = \mathbf{E}[e^{-sS_H}]$

$$r_L = 1 - \lambda \mathbf{E}[S_L]; \quad r_H = 1 - \lambda \mathbf{E}[S_H]; \quad \rho = \lambda(p \mathbf{E}[S_L] + (1 - p) \mathbf{E}[S_H])$$

429 We first present the theorems on asymptotic expressions for the mean busy periods. After pre-
 430 senting the theorems, we first present a brief proof sketch to elucidate how the theorems were
 431 derived, and then the detailed proofs. Theorem 6 considers the case $\lambda \mathbf{E}[S_H] > 1$, and Theorem 7
 432 considers the case $\lambda \mathbf{E}[S_H] < 1$.

Theorem 6. Let $r_H < 0$. That is, the system is under temporary overload during H states.

Case 1: $W_\alpha = \omega(1)$, $\Pr[\overline{W} = 0] = 0$:

$$\mathbf{E}[B_L(W_\alpha)] = \frac{\mathbf{E}[W_\alpha]}{1 - \rho} + o(W_\alpha)$$

$$\mathbf{E}[B_H(W_\alpha)] = \frac{\mathbf{E}[W_\alpha] + \frac{1 - \rho - r_H}{\alpha_H}}{1 - \rho} + o(\max\{W_\alpha, \alpha^{-1}\})$$

Case 2: $W_\alpha = \Theta(1)$:

$$\begin{aligned} \mathbf{E}[B_L(W_\alpha)] &= \frac{\mathbf{E}[\bar{W}]}{r_L} + p_{\text{switch}} \cdot (1 - Q_f) \frac{1 - \rho - r_H}{\alpha_H(1 - \rho)} + o(1) \\ \mathbf{E}[B_H(W_\alpha)] &= (1 - P_f) \cdot \frac{\mathbf{E}[\bar{W}] + \frac{1 - \rho - r_H}{\alpha_H}}{1 - \rho} + O(1) \end{aligned}$$

433 where, p_{switch} denotes the probability that the environment state switches to H before the busy
434 period started by \bar{W} in state L ends. We call this event a ‘switch’. The expression for p_{switch} is
435 given by $p_{\text{switch}} = \frac{\mathbf{E}[\bar{W}]_{\alpha_L}}{r_L} + o(\alpha)$. The quantity Q_f denotes the probability that, given a ‘switch’
436 occurs, the residual busy period is finite if the H state were to last indefinitely from then on:

$$Q_f = \tilde{V}(\lambda(1 - p_f)) + o(1)$$

437 where $\tilde{V}(\cdot)$ is given by ⁴: $\tilde{V}(s) = \frac{r_L \cdot \frac{1 - \tilde{W}(s)}{\mathbf{E}[\bar{W}]}}{s - \lambda(1 - \tilde{S}_L(s))}$, and $p_f \in (0, 1)$ solves the fixed point equation⁵:

438 $p_f = \tilde{S}_H(\lambda(1 - p_f))$.

439 The quantity P_f denotes the probability that the busy period started by \bar{W} during an H state is
440 finite if the H state were to last indefinitely and is given by $P_f = \tilde{W}(\lambda(1 - p_f))$.

Corollary 2. Consider the case $S_L \sim \text{Exp}(\mu_L)$ and $S_H \sim \text{Exp}(\mu_H)$, $\mu_L > \lambda > \mu_H$. Let B_s^c ($c, s \in \{L, H\}$) denote the busy period duration started by a class c job in environment state s . Then,

$$\begin{aligned} \mathbf{E}[B_L^L] &= \frac{1}{\mu_L - \lambda} \left(1 + \frac{1 - p}{p} \cdot \frac{\lambda - \mu_H}{\mu_L - \mu_H} \cdot \frac{\frac{\lambda}{\mu_H} - \rho}{1 - \rho} \right) + o(1); \\ \mathbf{E}[B_L^H] &= \frac{\mu_L}{\mu_H(\mu_L - \lambda)} \left(1 + \frac{1 - p}{p} (1 - Q_{fH}) \frac{\frac{\lambda}{\mu_H} - \rho}{1 - \rho} \right) + o(1) \end{aligned}$$

and:

$$\begin{aligned} \mathbf{E}[B_H^H] &= \left(1 - \frac{\mu_H}{\lambda} \right) \cdot \frac{\frac{\lambda}{\mu_H} - \rho}{\alpha_H(1 - \rho)} + o(\alpha^{-1}) \\ \mathbf{E}[B_H^L] &= \left(1 - \frac{\mu_L}{\mu_L + \lambda - \mu_H} \right) \cdot \frac{\frac{\lambda}{\mu_H} - \rho}{\alpha_H(1 - \rho)} + o(\alpha^{-1}). \end{aligned}$$

441 In the above, $1 - Q_{fH} = 1 - \tilde{V}_H(\lambda(1 - \phi_f))$, where $\phi_f = \frac{\mu_H}{\lambda}$, and $\tilde{V}_H(s) = \frac{\left(1 - \frac{\lambda}{\mu_L}\right) \left(\frac{\mu_H}{\mu_H + s}\right)}{1 - \frac{\lambda}{\mu_L} \left(\frac{\mu_L}{\mu_L + s}\right)}$.

⁴ The function $\tilde{V}(s)$ denotes the Laplace transform of the workload in the system just before the ‘switch’ event occurs. $\tilde{V}(s)$ is obtained as the Laplace transform of the stationary workload conditioned on server being busy in an $M/G/1$ with repeated vacations, with service distribution S_L and *i.i.d.* vacations distributed as \bar{W} .

⁵The quantity p_f denotes the probability that a busy period started by an H job in an H state is finite if the H state were to last indefinitely.

442 **Theorem 7.** Let $r_H > 0$. That is, the system is stable during H states.

443 **Case 1:** $W_\alpha = \omega(\alpha^{-1})$

$$\mathbf{E}[B_L(W_\alpha)] = \frac{\mathbf{E}[W_\alpha]}{1 - \rho} + o(W_\alpha) \quad ; \quad \mathbf{E}[B_H(W_\alpha)] = \frac{\mathbf{E}[W_\alpha]}{1 - \rho} + o(W_\alpha).$$

Case 2: $W_\alpha = \Theta(\alpha^{-1})$

$$\begin{aligned} \mathbf{E}[B_L(W_\alpha)] &= \frac{\mathbf{E}[W_\alpha]}{1 - \rho}(1 - u_\alpha) + \frac{\mathbf{E}[W_\alpha]}{r_L}u_\alpha + o(\alpha^{-1}) \\ \mathbf{E}[B_H(W_\alpha)] &= \frac{\mathbf{E}[W_\alpha]}{1 - \rho}(1 - u_\alpha) + \frac{\mathbf{E}[W_\alpha]}{r_H}u_\alpha + o(\alpha^{-1}) \end{aligned}$$

444 where $u_\alpha \equiv \left[\frac{1 - \widetilde{W}_\alpha \left(\frac{\alpha_L}{r_L} + \frac{\alpha_H}{r_H} \right)}{\mathbf{E}[W_\alpha] \left(\frac{\alpha_L}{r_L} + \frac{\alpha_H}{r_H} \right)} \right]$, $0 < u_\alpha < 1$, and $\lim_{\alpha \rightarrow 0} u_\alpha = u = \left[\frac{1 - \widetilde{W} \left(\frac{1-p}{r_L} + \frac{p}{r_H} \right)}{\mathbf{E}[\widetilde{W}] \left(\frac{1-p}{r_L} + \frac{p}{r_H} \right)} \right]$; and recall

445 $\widetilde{W} = \lim_{\alpha \rightarrow 0} \alpha W_\alpha$.

446 **Case 3:** $W_\alpha = o(\alpha^{-1})$

$$\mathbf{E}[B_L(W_\alpha)] = \frac{\mathbf{E}[W_\alpha]}{r_L} + o(W_\alpha); \quad \mathbf{E}[B_H(W_\alpha)] = \frac{\mathbf{E}[W_\alpha]}{r_H} + o(W_\alpha).$$

447 **Proof Sketch of Theorems 6 and 7:** Recall our fluid model, in which the workload decreases at
 448 deterministic rate r_L during the L states, and increases at rate $-r_H$ during the H states. We would
 449 like to believe that given an initial workload W_α , asymptotically the busy period started by W_α
 450 is the same as the duration of the busy period started by W_α under the fluid model. However, this is
 451 only partially true. When $W_\alpha = \Theta(\alpha^{-1})$, this asymptotic equivalence is justified by [4, Theorem
 452 1(b)] which proves the convergence of workload sample paths of the stochastic and fluid systems
 453 (although one needs to do a little more work to convert it to convergence of busy periods). For the
 454 remaining cases, we must consider the tree of events that may occur until each leaf corresponds
 455 to an empty system, or one with workload that is $\Theta(\alpha^{-1})$ so that we can apply [4, Theorem 1(b)].
 456 We describe this below.

457 **Case:** $W_\alpha = \omega(\alpha^{-1})$: In this case, the initial workload is of a higher order than the scale at which
 458 the system switches. Thus, asymptotically, the number of times the system switches states before
 459 W_α drains goes to ∞ as $\alpha \rightarrow 0$, and the workload sees the “average system” during its sojourn.
 460 Thus the mean busy period is $\frac{\mathbf{E}[W_\alpha]}{1 - \rho} + o(W_\alpha)$.

461 **Case:** $W_\alpha = \Theta(\alpha^{-1})$: As noted above, in this case from [4, Theorem 1(b)] asymptotically the
 462 mean busy period is given by the busy period under the fluid model. The final expressions are
 463 obtained by setting up and solving recurrences for the mean busy period under the fluid model.

464 **Remark 10:** When $r_H > 0$, the mean busy period started in state s is a convex combination of the
 465 busy period if the state s were to last indefinitely, and the busy period of the “average system”,
 466 with the coefficient being a function of the Laplace transform of the workload.

467 **Case:** $W_\alpha = o(\alpha^{-1})$, $r_H > 0$: In this case, the system is stable in both states. Consider a busy
 468 period starting in state L. If the L state were to last forever, the busy period would exactly be
 469 $\frac{\mathbf{E}[W_\alpha]}{r_L}$. However, since we may switch at rate $\Theta(\alpha)$, there is a $o(1)$ probability that the system
 470 switches to state H before the busy period finishes. If this switch were to happen, the remaining
 471 busy period would be stochastically bounded by a $\Theta(W_\alpha)$ random variable, as the system is
 472 always stable, thus giving a $o(W_\alpha)$ contribution to the overall busy period after multiplying by

473 the probability of switching. Thus asymptotically, the mean busy period started by W_α workload
474 in state L would be $\frac{\mathbf{E}[W_\alpha]}{r_L} + o(W_\alpha)$.

475 **Case:** $W_\alpha = \Theta(1)$, $r_H < 0$: This case is the most non-trivial of all, and clearly explains the
476 failure of fluid modeling of busy periods. First, consider a busy period started in state H by
477 $W_\alpha = \Theta(1)$ work. The fluid model would imply that the workload keeps increasing at rate $-r_H$
478 until the system switches to L. At this point we have $\Theta(\alpha^{-1})$ workload built up, and we could
479 apply [4, Theorem 1(b)]. However, given that we start with $\Theta(1)$ workload in state H (which is
480 in transient overload), there is still a constant ($\Theta(1)$) probability that the stochastic busy period
481 started by the $\Theta(1)$ workload is finite! This probability is denoted by P_f in Theorem 6, and given
482 that this event does not happen, we can use the fluid busy period expressions. Next, consider a
483 busy period started in state L by $W_\alpha = \Theta(1)$ work. In this case, with $\Theta(\alpha)$ probability (given by
484 p_{switch}), there is a class H arrival before the busy period ends. We are now in state H with $\Theta(1)$
485 workload (whose transform is given by $\tilde{L}(s) \cdot \tilde{S}_H(s)$). Given that a class H arrival happens, the
486 residual busy period (from our argument above) is $\Theta(\alpha^{-1})$. After multiplying it with p_{switch} , we
487 see that the contribution of this term to the overall busy period is $\Theta(1)$, and hence is of the same
488 asymptotic order as the duration of the busy period started in state L conditioned on it ending in
489 state L ($= \frac{\mathbf{E}[W_\alpha]}{r_L} + o(1)$). Therefore, we need to be precise with each of the terms involved, and
490 applying the fluid method does not yield the correct expressions. ■

491 **Proof of Theorem 6:**

492 **Case 1:** $W_\alpha = \omega(1)$, $\Pr[\bar{W} = 0] = 0$: We first show that under the fluid regime, the expres-
493 sions for the busy periods are as given. Then we will argue that when $W_\alpha = \omega(1)$, the fluid
494 approximation for the mean busy period is asymptotically the same as the stochastic busy period.
Let W_α be deterministic x , and $\tau_L \sim \text{Exp } \alpha_L$. Then we can write the following recurrence relation
for the fluid busy period started in L or H state by workload x .

$$\mathbf{E}[B_H(x)] = \frac{1}{\alpha_H} + \mathbf{E}\left[B_L\left(x - \frac{r_H}{\alpha_H}\right)\right]$$

$$\mathbf{E}[B_L(x)] = \mathbf{E}\left[\min\left\{\frac{x}{r_L}, \tau_L\right\}\right] + \mathbf{E}\left[B_H\left(x - r_L \min\left\{\frac{x}{r_L}, \tau_L\right\}\right) \cdot \mathbf{1}_{\{x > r_L \tau_L\}}\right].$$

495 Now we assume $\mathbf{E}[B_L(x)] = b_L x$ and $\mathbf{E}[B_H(x)] = a_H + b_H x$ for some constants b_L, a_H, b_H , and
496 then verify that these forms are indeed correct by identifying the unknown constants. Under the
497 assumed forms for fluid busy periods, the recurrences reduce to:

$$a_H + b_H x = \frac{1}{\alpha_H} + b_L x - b_L \frac{r_H}{\alpha_H}; \quad b_L x = \frac{1 - e^{-\frac{\alpha_L}{r_L} x}}{\alpha_L} + a_H (1 - e^{-\frac{\alpha_L}{r_L} x}) + b_H x - b_H r_L \frac{1 - e^{-\frac{\alpha_L}{r_L} x}}{\alpha_L}$$

498 Since the above equations should be satisfied for all x , we get $b_L = b_H = \frac{1}{1-\rho}$ and $a_H = \frac{1-\rho-r_H}{\alpha_H(1-\rho)}$
499 yielding the expressions in the theorem statement.

500 Now we verify that when $W_\alpha = \omega(1)$, the fluid busy period expressions are asymptotically cor-
501 rect. In the simple case $W_\alpha = \omega(\alpha^{-1})$, the system switches on a faster time-scale ($\Theta(\alpha^{-1})$) than
502 the initial amount of work ($\omega(\alpha^{-1})$). Thus this workload sees the “average” system (rather than
503 the transient system) and its busy period is simply $\frac{\mathbf{E}[W_\alpha]}{1-\rho} + o(W_\alpha)$.

504 When the workload is $\Theta(\alpha^{-1})$, then using [4], the sample paths of the stochastic system (scaled
505 by α) converge as $\alpha \rightarrow 0$ to the fluid sample path in the space $D[0, \infty)$. Thus, the mean busy
506 period of the stochastic system is within $o(\alpha^{-1})$ of the mean busy period of the fluid system.

507 Now consider the case $W_\alpha = \Theta(g(\alpha))$ where $g(\alpha) = \omega(1)$, but $g(\alpha) = o(\alpha^{-1})$ (e.g., $g(\alpha) = \frac{1}{\sqrt{\alpha}}$).
 508 **Subcase 1:** Busy period beginning in state H: We will show that even though the initial workload
 509 is $o(\alpha^{-1})$, since it is $\omega(1)$, with overwhelming probability, the sample paths will follow the fluid
 510 trajectory. Let $\widetilde{W}_\alpha(s) = \mathbf{E}[e^{-sW_\alpha}]$. Since reordering the jobs served in a busy period does not
 511 change the busy period duration, consider the case where the initial workload W_α is served first.
 512 If the H state were to last forever, the z -transform for the number of arrivals of class H jobs
 513 while workload W_α is served is given by $\widetilde{W}_\alpha(\lambda(1-z))$. The main idea is to show that since the
 514 H state is in overload, with probability tending to 1, at least one of the class H jobs will start a
 515 busy period that lasts until the end of the H state, whereby by the Strong Law of Large Numbers
 516 the accumulated workload will be $\Theta(\alpha^{-1})$. Consider the busy period that one class H job starts,
 517 provided the H state continues forever. The Laplace transform of the busy period in an $M/G/1$
 518 with only class H jobs, $\widetilde{B}_H(s)$, satisfies:

$$\widetilde{B}_H(s) = \widetilde{S}_H(s + \lambda(1 - \widetilde{B}_H(s))).$$

519 Since the $M/G/1$ is in overload, there is a constant probability that the busy period is infinite.
 520 The probability that the busy period is finite is obtained as

$$p_f = \lim_{s \rightarrow 0} \widetilde{B}_H(s).$$

521 Taking limit in the expression for $\widetilde{B}_H(s)$, we obtain:

$$p_f = \widetilde{S}_H(\lambda(1 - p_f))$$

522 The busy period started by W_α , given the H phase lasts forever, is finite if and only if the busy
 523 period started by each H arrival while W_α was served is finite. This probability, then is given by

$$\mathbf{Pr}[\text{busy period started during H is finite}] = \sum_{i=0}^{\infty} \mathbf{Pr}[i \text{ arrivals during } W_\alpha] \cdot p_f^i = \widetilde{W}_\alpha(\lambda(1-p_f)) \rightarrow 0.$$

524 The last fact is true since $\frac{W_\alpha}{g(\alpha)} \rightarrow \overline{W}$, $\widetilde{W}_\alpha(s) \rightarrow \widetilde{\overline{W}}(s \cdot g(\alpha)) \rightarrow 0$ as $\alpha \rightarrow 0$ ($\widetilde{\overline{W}}(s)$ is a decreas-
 525 ing function from 1 to 0, and $g(\alpha) = \omega(1)$). The fact that $\lim_{s \rightarrow \infty} \widetilde{\overline{W}}(s) = 0$ follows from the
 526 assumption $\mathbf{Pr}[\overline{W} = 0] = 0$.

527 Therefore, with probability approaching 1, the busy period started by W_α in phase H (under the
 528 assumption that the H phase lasts forever) is not finite. In other words, during the H phase, the
 529 workload increases asymptotically along the fluid trajectory, and then the system switches to the
 530 L phase. Since the work built up during the H state is $\Theta(\alpha^{-1})$, the workload follows the fluid
 531 trajectory after switching to the L state. Therefore, the expression for the mean busy period
 532 started in H phase by $\omega(1)$ work is indeed given by the mean busy period under the fluid regime
 533 within a $o(\max\{W_\alpha, \alpha^{-1}\})$ term.

534 **Subcase 2:** Busy period beginning in state L: Now we consider the case where the busy period
 535 starts in the L phase. If the L phase were to last forever, the workload in the system, scaled by
 536 $g(\alpha)$, would follow the fluid trajectory, and hence the mean busy period would be the mean busy
 537 period under the fluid regime within a $o(W_\alpha)$ term. However, with probability $\Theta(\alpha \cdot g(\alpha))$ the
 538 system switches to H state before the fluid workload reaches 0. Conditioned on switching to the
 539 H state before the period ends, the workload at the beginning of the H state is again $\Theta(g(\alpha))$.
 540 We have already argued above that subsequently the workload follows the fluid trajectory – and

541 the residual busy period will be $\Theta(\alpha^{-1})$ within an $o(\alpha^{-1})$ term. Therefore, the mean busy period
 542 started in L phase will be the mean busy period under the fluid regime, within a $o(W_\alpha)$ term.

543 **Case 2:** $W_\alpha = \Theta(1)$: We first consider the case where the busy period begins in the H state
 544 by workload \bar{W} with Laplace transform $\widetilde{W}(s)$. As we have argued above, since the H state is
 545 in overload, there is a constant probability that the busy period does not end before the system
 546 switches to the L state. This probability is given by $1 - P_f$ where,

$$P_f = \widetilde{W}(\lambda(1 - p_f))$$

547 and p_f is the solution to the fixed point equation $p_f = \widetilde{S}_H(\lambda(1 - p_f))$. P_f denotes the proba-
 548 bility that a busy period started by work \bar{W} in the $M/G/1$ under overload is finite, and p_f is the
 549 probability that a busy period started by a single class H job is finite.

550 Given that the busy period does not end before the system switches, the work that builds up in
 551 the system is given by $\tau_H(\frac{\lambda}{\mu_H} - 1) + o(\alpha^{-1})$ where τ_H denotes the duration of the H state and
 552 is $\Theta(\alpha^{-1})$. We can thus apply the previous case and conclude that the mean busy period in this
 553 case, that is with probability $1 - P_f$, is given by $\frac{1}{\alpha_H} - \frac{r_H}{\alpha_H(1-p)}$. In simpler terms, we are starting
 554 the busy period with $\Theta(1)$ work in the H state. With $\Theta(1)$ probability, the busy period does not
 555 end in the H phase, in which case we start the subsequent L state with $\Theta(\alpha^{-1})$ work, with an
 556 overall contribution to the mean busy period of $\Theta(\alpha)$. If however, the original busy period ends
 557 in the H state itself, then this event contributes a $\Theta(1)$ term and hence is asymptotically negligible
 558 compared to the contribution of the event where the busy period does not end in the H state.

559 Now we consider the case where the busy period begins in an L state. Again, we have two cases
 560 – either the busy period ends in the L state itself, or the system switches to an H state before the
 561 busy period ends. If the busy period ends in the L state, an event which happens with probability
 562 $1 - \Theta(\alpha)$, then the mean busy period conditioned on this event is given by $\frac{E[\bar{W}]}{r_L}$. However,
 563 the system can switch with probability $\Theta(\alpha)$, and the contribution of the residual busy period
 564 conditioned on this event can be $\Theta(\alpha^{-1})$ (from the previous subcase). Therefore, this event also
 565 contributes a $\Theta(1)$ term to the mean busy period, and we handle this event next.

566 Consider an $M/G/1$ busy period started by work \bar{W} . We let this $M/G/1$ evolve in the L state, and
 567 consider an independent Poisson(α_L) marking process. Our aim is to find the workload in the
 568 $M/G/1$ when the first mark arrives during the busy period. The probability that no mark arrives
 569 is given by $1 - \frac{E[\bar{W}]\alpha_L}{r_L}$, which we denote by $1 - p_{switch}$ in the theorem statement. Thus, with
 570 probability p_{switch} , at least one mark arrives, or equivalently, the environment processes switches
 571 before the busy period ends and hence the busy period now evolves in the H state.

572 The subsequent busy period (that which evolves after the system switches to H) is given by the
 573 the busy period that starts in H state with work $\widetilde{V}(s)$, where $\widetilde{V}(s)$ denotes the transform of the
 574 work that is seen by the Poisson(α_L) marking process *conditioned on being the first mark of a*
 575 *busy period*. We will now argue that this is asymptotically given by the stationary work in an
 576 $M/G/1$ conditioned on the server being busy, with exceptional service distribution for the job
 577 that starts the busy period given by \bar{W} , and service distribution S_L . We first note that if we
 578 have such an $M/G/1$ where we consider the distribution of work seen by all marks, then this
 579 is indeed the stationary work conditioned on the server being busy, and hence is given by the
 580 stationary delay seen by arrivals finding the server busy in an $M/G/1$ system with special first

581 service (this expression, $\widetilde{V}(s) = \frac{r_L \cdot \frac{1 - \widetilde{W}(s)}{E[\bar{W}]}}{s - \lambda(1 - S_L(s))}$, is given in the theorem statement; see [26] or [15,
 582 Appendix B] for proof). However, we are interested in the work that the first mark sees in a

583 busy period, call this W_1 . We will argue that as the probability of marking goes to 0, the work
 584 seen by the first mark converges in distribution to the stationary work conditioned on the server
 585 being busy (and that this sequence of random variables remains uniformly integrable so that the
 586 Laplace transforms converge). We first note that the work seen by the first mark is stochastically
 587 bounded above by the supremum of the work in a busy period started by work \bar{W} , denote this
 588 by W_1^* . Further, conditioned on a second marked arrival, we can upper bound the work that this
 589 mark sees by the supremum of the work in the busy period started by W_1^* (which is an upper
 590 bound on the work after the arrival of the first mark), denote this by W_2^* . Similarly, we can obtain
 591 an upper bound on the work seen by the n th marked arrival in a busy period. We also have the
 592 trivial lower bound of 0 on the work seen by the n th marked arrival in a busy period. Note that
 593 both these upper and lower bounds are independent of the marking probability. Let p_i denote the
 594 probability that there are i marked arrivals in a busy period. We can thus sandwich the stationary
 595 work of the $M/G/1$ conditioned on it being busy between $\frac{p_1 \cdot W_1}{\sum_{i=1}^{\infty} p_i}$ and $\frac{p_1 \cdot W_1 + \sum_{i=2}^{\infty} p_i \cdot W_i^*}{\sum_{i=1}^{\infty} p_i}$. However, as
 596 the marking probability ($\Theta(\alpha)$) goes to 0, $p_i \sim \Theta(\alpha^i)$. Therefore, W_1 converges to the stationary
 597 work in the $M/G/1$ with special service, conditioned on server being busy. ■

598 Proof of Theorem 7:

599 Recall that the work is decreasing during both the L and H states. There is a negative drift of
 600 $r_L = 1 - \frac{\lambda}{\mu_L}$ during the L phase and a negative drift of $r_H = 1 - \frac{\lambda}{\mu_H}$ during the H phase.

601 **Case 1:** $W_\alpha = \omega(\alpha^{-1})$: As in the proof of Theorem 6, since the system switches at a faster time
 602 scale ($\Theta(\alpha^{-1})$) than the initial work ($\omega(\alpha^{-1})$), the work during its sojourn sees an average system,
 603 and hence the busy period is $\frac{\mathbf{E}[W_\alpha]}{1-\rho} + o(W_\alpha)$.

604 **Case 2:** $W = \Theta(\alpha^{-1})$: We begin by noting that since the initial work is $\Theta(\alpha^{-1})$, the workload
 605 trajectory of the stochastic system, scaled by α , converges to the fluid trajectory. Hence the busy
 606 period of the stochastic system is given by the fluid busy period and an additional $o(\alpha^{-1})$ term.

We now set up the recurrences for busy periods started by deterministic work x during the H and
 L phases under the fluid regime:

$$\mathbf{E}[B_H(x)] = \mathbf{E}\left[\min\left\{\frac{x}{r_H}, \tau_H\right\}\right] + \mathbf{E}\left[B_L\left(x - r_H \min\left\{\frac{x}{r_H}, \tau_H\right\}\right) \cdot \mathbf{1}_{\{x > r_H \tau_H\}}\right]$$

$$\mathbf{E}[B_L(x)] = \mathbf{E}\left[\min\left\{\frac{x}{r_L}, \tau_L\right\}\right] + \mathbf{E}\left[B_H\left(x - r_L \min\left\{\frac{x}{r_L}, \tau_L\right\}\right) \cdot \mathbf{1}_{\{x > r_L \tau_L\}}\right]$$

607 where τ_H is an $\text{Exp}(\alpha_H)$ random variable and τ_L is an $\text{Exp}(\alpha_L)$ random variable.

608 We now guess and verify that $\mathbf{E}[B_H(x)]$ and $\mathbf{E}[B_L(x)]$ have the following function form:

$$B_i(x) = a_i + b_i x + c_i e^{-\left(\frac{\alpha_L}{r_L} + \frac{\alpha_H}{r_H}\right)x}$$

where a_i, b_i and $c_i, i \in \{L, H\}$, are constants to be determined. The ‘guess’ is in fact an educated
 attempt arrived at by exact analysis of the mean busy period started by n jobs in an alternate
 discrete system which is identical on fluid scale to the system we want to analyze, but with 0
 arrival rate. Since $B_i(0) = 0$, we have $a_i = -c_i$. Since the Laplace transform for $x - r_i \min\left\{\frac{x}{r_i}, \tau_i\right\}$

is $\mathbf{E}\left[e^{-s\left(x - \min\left\{\frac{x}{r_i}, \tau_i\right\}\right)}\right] = \frac{se^{-\frac{\alpha_i}{r_i}x} - \frac{\alpha_i}{r_i}e^{-sx}}{s - \frac{\alpha_i}{r_i}}$ and $\mathbf{E}\left[\min\left\{\frac{x}{r_i}, \tau_i\right\}\right] = \frac{1 - e^{-\frac{\alpha_i}{r_i}x}}{\alpha_i}$, our recurrences become:

$$a_L + b_L x + c_L e^{-\left(\frac{\alpha_L}{r_L} + \frac{\alpha_H}{r_H}\right)x} = \frac{1 - e^{-\frac{\alpha_L}{r_L}x}}{\alpha_L} + a_H + b_H \left(x - \frac{1 - e^{-\frac{\alpha_L}{r_L}x}}{\frac{\alpha_L}{r_L}}\right) + c_H \left(\frac{\left(\frac{\alpha_L}{r_L} + \frac{\alpha_H}{r_H}\right)e^{-\frac{\alpha_L}{r_L}x} - \frac{\alpha_L}{r_L}e^{-\left(\frac{\alpha_L}{r_L} + \frac{\alpha_H}{r_H}\right)x}}{\frac{\alpha_H}{r_H}}\right)$$

$$a_H + b_H x + c_H e^{-\left(\frac{\alpha_L + \alpha_H}{r_L + r_H}\right)x} = \frac{1 - e^{-\frac{\alpha_H}{r_H}x}}{\alpha_H} + a_L + b_L \left(x - \frac{1 - e^{-\frac{\alpha_H}{r_H}x}}{\frac{\alpha_H}{r_H}} \right) + c_L \left(\frac{\left(\frac{\alpha_L + \alpha_H}{r_L + r_H}\right) e^{-\frac{\alpha_H}{r_H}x} - \frac{\alpha_H}{r_H} e^{-\left(\frac{\alpha_L + \alpha_H}{r_L + r_H}\right)x}}{\frac{\alpha_L}{r_L}} \right).$$

Since the above equalities hold for all x , together with $a_i = -c_i$, we get:

$$\begin{aligned} b_L = b_H &= \left(\frac{\frac{r_L}{\alpha_L} + \frac{r_H}{\alpha_H}}{\frac{1}{\alpha_L} + \frac{1}{\alpha_H}} \right)^{-1} = \frac{1}{1 - \rho}, \\ -a_L = c_L &= \frac{r_L - r_H}{\alpha_L \alpha_H \left(\frac{r_L}{\alpha_L} + \frac{r_H}{\alpha_H} \right)^2} \cdot \frac{r_H}{\alpha_H}, \\ -a_H = c_H &= -\frac{r_L - r_H}{\alpha_L \alpha_H \left(\frac{r_L}{\alpha_L} + \frac{r_H}{\alpha_H} \right)^2} \cdot \frac{r_L}{\alpha_L}. \end{aligned}$$

Therefore the expected busy period started by a work of size x during L and H phases, respectively, can be expressed in the following convenient/intuitive form:

$$\mathbf{E}[B_L(x)] = \frac{x}{1 - \rho} - \left(\frac{x}{1 - \rho} - \frac{x}{r_L} \right) \cdot \left[\frac{1 - e^{-\left(\frac{\alpha_L + \alpha_H}{r_L + r_H}\right)x}}{\left(\frac{\alpha_L + \alpha_H}{r_L + r_H}\right)x} \right] \quad (\text{B.1})$$

$$\mathbf{E}[B_H(x)] = \frac{x}{1 - \rho} - \left(\frac{x}{1 - \rho} - \frac{x}{r_H} \right) \cdot \left[\frac{1 - e^{-\left(\frac{\alpha_L + \alpha_H}{r_L + r_H}\right)x}}{\left(\frac{\alpha_L + \alpha_H}{r_L + r_H}\right)x} \right] \quad (\text{B.2})$$

609 which show that $\mathbf{E}[B_L(x)]$ and $\mathbf{E}[B_H(x)]$ are weighted averages of the busy periods of the $\alpha \rightarrow$
 610 0 and $\alpha \rightarrow \infty$ cases. Taking expectation over x (which is distributed as W_α), we obtain the
 611 expressions given in the theorem.

612 **Case 3:** $W_\alpha = o(\alpha^{-1})$: Since the system is stable during both the L and H states, the busy period
 613 is $\Theta(W_\alpha)$ (being upper bounded by the busy period started by W_α in an $M/G/1$ with service
 614 distribution S_H). Suppose the busy period starts in the L state. If the L state were to last forever,
 615 the busy period would indeed be $\frac{\mathbf{E}[W_\alpha]}{r_L}$. Now either the system switches to the H state before
 616 this busy period ends, and this event happens with probability $1 - o(1)$. In this case, the length
 617 of the busy period conditioned on it being smaller than $\text{Exp}(\alpha_L)$ will be $\frac{\mathbf{E}[W_\alpha]}{r_L} + o(W_\alpha)$ since
 618 $W_\alpha = o(\alpha^{-1})$. However, if the system switches before the busy period ends, which happens with
 619 probability $o(1)$, the residual busy period is still $\Theta(W_\alpha)$. The overall contribution of the second
 620 event to the mean busy period started by W_α is $o(W_\alpha)$. By law of total probability, the mean busy
 621 period started in L phase is $\frac{\mathbf{E}[W_\alpha]}{r_L} + o(W_\alpha)$.

622 The proof for busy periods started during H phases is identical. ■

623 References

- 624 [1] <http://www.cs.huji.ac.il/labs/parallel/workload/>.
 625 [2] I. J. B. F. Adan and V. G. Kulkarni. Single-server queue with Markov-dependent inter-arrival and service times.
 626 *QUESTA*, 45:113–134, 2003.
 627 [3] S. C. Borst, O. J. Boxma, and M. B. Combé. Collection of customers: a correlated $M/G/1$ queue. In *SIGMET-*
 628 *RICS/Performance*, pages 47–59, New York, NY, USA, 1992. ACM.
 629 [4] G. L. Choudhury, A. Mandelbaum, M. I. Reiman, and W. Whitt. Fluid and diffusion limits for queues in slowly
 630 changing environments. *Stoch. Mod.*, 13:121–146, 1997.

- 631 [5] I. Cidon, R. Gurin, A. Khamisy, and M. Sidi. Analysis of a correlated queue in a communication system. In
632 *INFOCOM'93*, pages 209–216, 1993.
- 633 [6] J. Cohen. *The single server queue*. North Holland, 1969.
- 634 [7] R. Conway, W. Maxwell, and M. Miller. *Theory of Scheduling*. Addison-Wesley, 1967.
- 635 [8] M. E. Crovella and A. Bestavros. Self-similarity in World Wide Web traffic: Evidence and possible causes. In
636 *ACM SIGMETRICS'96*, pages 160–169, May 1996.
- 637 [9] A. Erramilli, O. Narayan, and W. Willinger. Experimental queueing analysis with long-range dependent packet
638 traffic. *IEEE/ACM Trans. on Networking*, 4:209–223, 1996.
- 639 [10] D. G. Feitelson. Packing schemes for gang scheduling. In *IPPS*, pages 89–110, London, UK, 1996. Springer-
640 Verlag.
- 641 [11] D. G. Feitelson. Locality of sampling and diversity in parallel system workloads. In *Proceedings of the 21st annual*
642 *International Conference on Supercomputing*, pages 53–63, New York, NY, USA, 2007. ACM.
- 643 [12] K. Fendick, V. Saksena, and W. Whitt. Dependence in packet queues. *IEEE Trans. Commun.*, 37:1173–1183, 1989.
- 644 [13] H. J. Fowler, W. E. Leland, and B. Bellcore. Local area network traffic characteristics, with implications for
645 broadband network congestion management. *IEEE Journal on Selected Areas in Communications*, 9:1139–1149,
646 1991.
- 647 [14] S. Ghosh and M. Squillante. Analysis and control of correlated web server queues. *Computer Communications*,
648 27(18):1771–1785, 2004.
- 649 [15] V. Gupta, M. Burroughs, and M. Harchol-Balder. Analysis of scheduling policies under correlated job sizes. Tech-
650 nical Report CMU-CS-10-107, School of Computer Science, Carnegie Mellon University, 2010.
- 651 [16] H. Li, D. Groep, and L. Wolters. Workload characteristics of a multi-cluster supercomputer. pages 176–193.
652 Springer Verlag, 2004.
- 653 [17] M. Livny, B. Melamed, and A. K. Tsiolis. The impact of autocorrelation on queuing systems. *Manage. Sci.*,
654 39(3):322–339, 1993.
- 655 [18] N. Mi, G. Casale, and E. Smirni. Scheduling for performance and availability in systems with temporal dependent
656 workloads. In *DSN'08*, pages 336–345, 2008.
- 657 [19] N. Mi, G. Casale, Q. Zhang, A. Riska, and E. Smirni. Autocorrelation-driven load control in distributed systems.
658 In *MASCOTS'09*, 2009.
- 659 [20] V. Paxson and S. Floyd. Wide area traffic: the failure of Poisson modeling. *IEEE/ACM Transactions on Networking*,
660 3(3):226–244, 1995.
- 661 [21] R. Richter, J. G. Shanthikumar, and G. Yamazaki. On extremal service disciplines in single-stage queueing systems.
662 *J. Appl. Probab.*, 27(2):409–416, 1990.
- 663 [22] A. Riska, M. Squillante, S.-Z. Yu, Z. Liu, and L. Zhang. Matrix-analytic analysis of a *MAP/PH/1* queue fitted to
664 web server data. *Matrix-Analytic Methods: Theory and Applications*, pages 335–356, 2002.
- 665 [23] E. Smirni, Q. Zhang, N. Mi, A. Riska, and G. Casale. New results on the performance effects of autocorrelated
666 flows in systems. In *IEEE IPDPS'07*, pages 1–6, 2007.
- 667 [24] B. Song, C. Ernemann, and R. Yahyapour. Parallel computer workload modeling with markov chains. In *Proc. of*
668 *the 10th Job Scheduling Strategies for Parallel Processing (JSSPP)*, pages 47–62. Springer, 2004.
- 669 [25] M. S. Squillante, D. D. Yao, and L. Zhang. Internet traffic: periodicity, tail behavior, and performance implications.
670 *System performance evaluation: methodologies and applications*, pages 23–37, 2000.
- 671 [26] H. Takagi. *Queueing Analysis, Vol. 1: Vacation and Priority Systems*. North-Holland, 1991.
- 672 [27] E. van Doorn and J. Regterschot. Conditional PASTA. *Oper. Res. Lett.*, 7:229–232, 1988.
- 673 [28] Q. Zhang, N. Mi, A. Riska, and E. Smirni. Load unbalancing to improve performance under autocorrelated traffic.
674 In *ICDCS'06*, Lisboa, Portugal, 2006.